Inorganic Chemistry

Article

pubs.acs.org/IC

Synthesis and Photochemical Properties of pH Responsive Tris-Cyclometalated Iridium(III) Complexes That Contain a Pyridine Ring on the 2-Phenylpyridine Ligand

Akihiro Nakagawa,[†] Yosuke Hisamatsu,[†,‡] Shinsuke Moromizato,[†] Masahiro Kohno,[§] and Shin Aoki*[,†,‡]

[†]Faculty of Pharmaceutical Sciences and [‡]Center for Technologies against Cancer, Tokyo University of Science, 2641 Yamazaki, Noda, Chiba 278-8510, Japan

[§]Graduate School of Bioscience and Biotechnology, Tokyo Institute of Technology, 4259 Nagatsuta-cho, Midori-ku, Yokohama, Kanagawa 226-8503, Japan

Supporting Information

ABSTRACT: In our previous publication, it was reported that *fac*-Ir(atpy)$_3$ **3** (atpy = 2-(5′-amino-4′-tolyl)pyridine), which contains three amino groups at the 5′-position of the atpy ligands, exhibits a pH-dependent change in the color of the emitted radiation. Aqueous solution of **3** shows a weak red emission (at around 613 nm) under neutral or basic conditions, but the emission color changes to green (at around 530 nm) under acidic conditions, where the NH_2 group is protonated to become an electron-withdrawing $(NH_3)^+$ group. In this manuscript, we report on the preparation of some new pH-responsive Ir(III) complexes; *fac*-Ir(4Pyppy)$_3$ **5** and *fac*-Ir(3Pyppy)$_3$ **6** that contain three pyridyl groups at the 5′-position of the 2-phenylpyridine (ppy) ligand, and Ir(4Pyppym)$_3$ **7** and Ir(3Pyppym)$_3$ **8** that contain a pyridyl group at the same position of the 2-phenylpyrimidine (ppym) ligand. The introduction of three pyridyl groups on iodinated Ir(ppy)$_3$ and Ir(ppym)$_3$ was achieved via Suzuki−Miyaura cross-coupling reaction assisted by microwave irradiation. Solutions of the acid-free Ir(III) complexes **5**, **6**, **7**, and **8** showed a strong green emission (at around 500 nm) in dimethylsulfoxide (DMSO). Protonation of three pyridyl groups of **5** and **7** causes a significant red-shift in the emission wavelength (at around 600 nm) with a decrease in emission intensity. The pH-dependent emission change of these complexes is also discussed. The generation of singlet oxygen ($^1O_2$) by the photoirradiation of the Ir complexes **5** and **6** was evidenced by the decomposition of 1,3-diphenylisobenzofuran (DPBF), the oxidation of thioanisole, and the oxidation of 2,2,5,5-tetramethyl-3-pyrroline-3-carboxamide (TPC). The induction of necrosis-like cell death of HeLa-S3 cells upon photoirradiation of **5** at 465 nm is also reported.

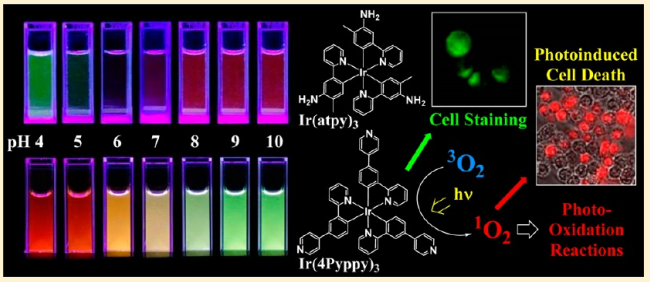

INTRODUCTION

Cyclometalated iridium(III) complexes such as *fac*-Ir(ppy)$_3$ **1** (ppy = 2-phenylpyridine) and *fac*-Ir(tpy)$_3$ **2** (tpy = 2-(4′-tolylpyridine)) (Chart 1) have unique photophysical properties as phosphorescence materials, since they possess high luminescent quantum yields and have relatively longer phosphorescent lifetimes ($\tau \sim \mu$s) than the fluorescence analogue.[1] The highly efficient spin−orbit coupling (SOC) of Ir(III) metal ion in the complexes promote intersystem crossing (ISC) from the singlet state to the triplet state. As a result, the complexes exhibit strong phosphorescence even at room temperature.[2] Furthermore, the photochemical properties (e.g., emission wavelength) of these materials can be tuned by appropriate modification of the ligand units.[3] Because of these excellent and tunable photochemical properties, Ir(III) complexes are utilized as phosphorescent emitters in organic light-emitting diodes (OLEDs),[4] chemosensors,[5] photoredox catalysis,[6] and as luminescent probes for biological systems.[7]

We recently reported on the regioselective substitution reactions of **1** and **2** at the 5′-position (*p*-position with respect to the C−Ir bond) on the ppy or tpy portions.[8−10] In our previous publication, it was reported that *fac*-Ir(atpy)$_3$ **3** (atpy =

Chart 1

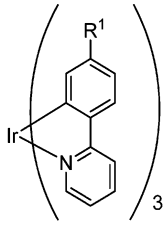

1: R^1 = H (*fac*-Ir(ppy)$_3$)
2: R^1 = Me (*fac*-Ir(tpy)$_3$)

Received: September 20, 2013
Published: December 16, 2013

2-(5′-amino-4′-tolyl)pyridine), which contains three amino groups at the 5′-position of the atpy ligands, exhibits a pH-dependent change in the color of the emitted radiation (Chart 2).[8,11] Aqueous solution of **3** shows a weak red emission (at

Chart 2

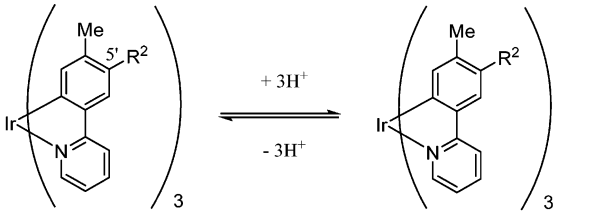

3: $R^2 = NH_2$ ($Ir(atpy)_3$) Em 600 nm at neutral~basic pH
4: $R^2 = NEt_2$ ($Ir(deatpy)_3$) Negligible Em at neutral~basic pH
H_3·**3**: $R^2 = NH_3^+$ (H_3·$Ir(atpy)_3$) Em 530 nm at acidic pH
H_3·**4**: $R^2 = NHEt_2^+$ (H_3·$Ir(deatpy)_3$) Em 490 nm at acidic pH

around 613 nm) under neutral or basic conditions, but the emission color changes to green (at around 530 nm) under acidic conditions, because the electron-donating NH_2 group is protonated, thus becoming an electron-withdrawing $(NH_3)^+$ group. Furthermore, the emission intensity of the tris-(diethylamino) derivative, *fac*-Ir(deatpy)$_3$ **4** (deatpy = 2-(5′-*N*,*N*-diethylamino-4′-tolyl)pyridine) undergoes a considerable change in going from neutral to a slightly acidic pH (pH 6.5–7.4).[12] Results of cellular imaging studies of HeLa-S3 cells indicate that **4** is useful for the selective staining of lysosomes, an acidic organelle in cells. Moreover, **4** is capable of generating $^1O_2$ from $^3O_2$ by photoirradiation, resulting in necrosis-like cell death.[12,13]

In an extension of our previous work, we were prompted to investigate the pH-responsive photochemical properties of tris-cyclometalated Ir(III) complexes having three pyridine rings at the 5′-positions, *fac*-Ir(4Pyppy)$_3$ **5** (4Pyppy = 2-(5′, 4″-pyridylphenyl)-pyridine) and *fac*-Ir(3Pyppy)$_3$ **6** (3Pyppy =2-(5′, 3″-pyridylphenyl)pyridine) (Chart 3).[14] The preliminary results of Density Functional Theory (DFT) calculations[15] suggested that the protonation of three pyridyl groups of **5** and **6** narrows the energy gap between the highest occupied

Chart 3

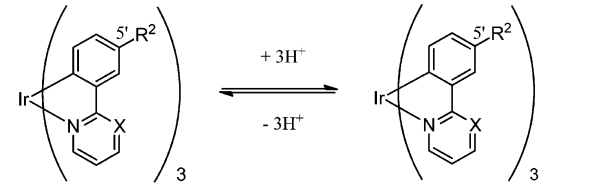

5: X = CH, R^2 = (Ir(4Pyppy)$_3$) H_3·**5**: R^2 = (Ir(4PyHppy)$_3$)
6: X = CH, R^2 = (Ir(3Pyppy)$_3$) H_3·**6**: R^2 = (Ir(3PyHppy)$_3$)
7: X = N, R^2 = (Ir(4Pyppym)$_3$) H_3·**7**: R^2 = (Ir(4PyHppym)$_3$)
8: X = N, R^2 = (Ir(3Pyppym)$_3$) H_3·**8**: R^2 = (Ir(3PyHppym)$_3$)

molecular orbital (HOMO) and the lowest unoccupied molecular orbital (LUMO) and induces a red-shift in the emission wavelength (see below),[16] which may bring about different photochemical behaviors from those of **3** and **4**.

In this manuscript, we report on the design, synthesis, and the photochemical properties of new Ir(III) complexes, **5** and **6**.[17] They exhibited a reversible, pH-dependent change in their emission based on protonation and deprotonation of the nitrogen atoms on the pyridine rings. As expected, the Ir(III) complex **5** showed a green colored emission under neutral and basic conditions and a weak red emission at acidic pH, which is opposite to that for **3** and **4**. Furthermore, we synthesized the Ir(III) complexes **7** and **8** containing 2-phenylpyrimidine (ppym) ligands (Chart 3), which were predicted to be more soluble in water than **5** and **6**, and measured their phosphorescence behavior. In addition, singlet oxygen ($^1O_2$)[18] was efficiently generated by the photoirradiation of **5** and **6**, as evidenced by the decomposition of 1,3-diphenylisobenzofuran (DPBF), the oxidation of thioanisole, and the formation of a nitroxide radical from 2,2,5,5-tetramethyl-3-pyrroline-3-carboxamide (TPC). The photoinduced cell death of HeLa-S3 cells was also observed and is discussed below.

EXPERIMENTAL SECTION

General Information. $IrCl_3·3H_2O$ was purchased from the KANTO CHEMICAL Co. and bis-(triphenylphosphine)palladium(II) dichloride was purchased from SIGMA-Aldrich. 4-Pyridine-boronic acid, 3-pyridine-boronic acid, [1,1′-bis(diphenylphosphino)ferrocene]-dichloropalladium(II) and organic solvents for spectroscopic analysis were purchased from WAKO CHEMICALS Co., Ltd. All reagents and solvents were of the highest commercial quality and were used without further purification, unless otherwise noted. Anhydrous CH_2Cl_2, MeCN, and dimethylformamide (DMF) were obtained by distillation from CaH_2. All aqueous solutions were prepared using deionized water. Ir(ppy)$_3$ **1**[19] and Ir(Ippy)$_3$ **10**[8] were prepared according to a literature procedure. Melting points were measured on a YANACO MP-33 Micro Melting Point Apparatus and are uncorrected. For measurement of UV/vis and luminescence spectra in aqueous solution at given pHs, buffer solutions (CAPS, pH 10.0; CHES, pH 9.0; EPPS, pH 8.0; HEPES, pH 7.4 and 7.0; MES, pH 6.0, 5.0 and 4.0) were used. Good's buffer reagents (Dojindo) were obtained from commercial sources: MES (2-morpholinoethanesulfonic acid, pK_a = 6.15), HEPES (2-[4-(2-hydroxyethyl)-1-piperazinyl]ethanesulfonic acid, pK_a = 7.5), EPPS (3-[4-(2-hydroxyethyl)-1-piperazinyl]propanesulfonic acid, pK_a = 8.0), CHES (2-(cyclohexylamino)ethanesulfonic acid, pK_a = 9.5), CAPS (3-(cyclohexylamino)propanesulfonic acid, pK_a = 10.4). IR spectra were recorded on a Perkin-Elmer FTIR-Spectrum 100 (ATR). ^1H NMR (400 MHz) was recorded on a JEOL Lambda 400 spectrometer, and ^1H NMR (300 MHz) was recorded on a JEOL Always 300 spectrometer. Elemental analyses were performed on a Perkin-Elmer CHN 2400 analyzer. Thin-layer chromatography (TLC) was performed using a Merck 5554 (silica gel) TLC plate. Silica gel column chromatographies were performed using Fuji Silysia Chemical FL-100D. Emission lifetimes were measured on a TSP-1000 (Unisoku Co., Ltd.). DFT and time-dependent DFT (TD-DFT) calculations were also carried out using the Gaussian03 program (B3LYP, the LanL2DZ basis set for the Ir atom and the 6-31G basis sets for the H, C, N atoms).[9,15] The HOMO and LUMO energies were obtained by single point calculations of the optimized Ir complexes.

Microwave reactions were conducted using the Discover Bench-Mate microwave apparatus (CEM Corporation) and the corresponding vials. The reactions were performed in glass vials (capacity 10 mL) sealed with a septum, under magnetic stirring. The temperature of the reaction mixture was monitored using a calibrated infrared temperature control mounted under the reaction vial. In a typical procedure, the reaction mixtures were irradiated in a sealed vial at 120 °C for 30 min (200 W).

dx.doi.org/10.1021/ic402387b | *Inorg. Chem.* 2014, 53, 409–422

*fac-Tris[2-(5′-(p-pyridyl)phenyl)pyridine]iridium(III) (**5**).* A mixture of compound **10**[8] (19.7 mg, 19.0 μmol), H_2O (1.0 mL), 4-pyridineboronic acid (15.4 mg, 126 μmol), Cs_2CO_3 (43.4 mg, 123 μmol), and $PdCl_2(PPh_3)_2$ (4.3 mg, 30 mol %) in distilled DMF (5.0 mL) was added to a 10 mL microwave vial. The reactor was subjected to microwave irradiation at 120 °C for 30 min.[20] After cooling to room temperature, H_2O (10 mL) and a few drops of 10 N NaOH aq. were then added. The organic layer was extracted with $CHCl_3$ (30 mL four times), dried over Na_2SO_4, and concentrated under reduced pressure. The resulting residue was purified by silica gel column chromatography (CH_2Cl_2 to CH_2Cl_2/MeOH = 20:1) and recrystallized from $CHCl_3$/hexane to afford **5** as a yellow powder (7.1 mg, 42% yield); mp >300 °C. IR (ATR): ν = 3031, 1590, 1561, 1474, 1425, 1259, 1162, 1072, 1027, 993, 810, 786, 753, 722 cm^{-1}. ^1H NMR (300 MHz, $CDCl_3$/TMS): δ = 8.58 (d, J = 4.7 Hz, 6H), 8.06 (d, J = 8.4 Hz, 3H), 7.97 (s, 3H), 7.72 (t, J = 7.9 Hz, 3H), 7.61 (d, J = 5.1 Hz, 3H), 7.54 (d, J = 4.7 Hz, 6H), 7.19 (d, J = 8.1 Hz, 3H), 7.02 (d, J = 7.8 Hz, 3H), 7.01 (t, J = 7.8 Hz, 3H) ppm. ESI-MS: m/z Calcd. for $C_{48}H_{34}IrN_6$ [M^+]: 885.2445, Found: 885.2436. Anal. Calcd. for $C_{48}H_{33}IrN_6{\cdot}3H_2O{\cdot}2CHCl_3$: C, 50.94; H, 3.51; N, 7.13. Found: C, 50.64; H, 3.57; N, 7.00.

*fac-Tris[2-(5′-(m-pyridyl)phenyl)pyridine]iridium(III) (**6**).* A mixture of compound **10**[8] (21.1 mg, 20.4 μmol), H_2O (0.4 mL), 3-pyridineboronic acid (15.3 mg, 124 μmol), argon-saturated aqueous 2 M KF (0.6 mL), and $PdCl_2$(dppf) (12.1 mg, 60 mol %) in distilled DMF (5.0 mL) was added to a 10 mL microwave vial.[21] The reactor was subjected to microwave irradiation at 120 °C for 45 min.[20] After cooling to room temperature, H_2O (10 mL) and a few drops of 10 N NaOH aq. were then added. The organic layer was extracted with $CHCl_3$ (30 mL four times), dried over Na_2SO_4 and concentrated under reduced pressure. The resulting residue was purified by silica gel column chromatography (CH_2Cl_2 to CH_2Cl_2/MeOH = 30:1) and the resulting material was recrystallized from CH_2Cl_2/EtOH/hexane to afford **6** as a yellow powder (8.5 mg, 47% yield); mp >300 °C. IR (ATR): ν = 3336, 1591, 1472, 1418, 1256, 1187, 1158, 1073, 1027, 889, 842, 802, 785, 753, 708 cm^{-1}. ^1H NMR (300 MHz, $CDCl_3$/TMS): δ = 8.89 (d, J = 2.1 Hz, 3H), 8.51 (dd, J = 1.8, 4.8 Hz, 3H), 8.04 (d, J = 8.4 Hz, 3H), 7.90 (m, 6H), 7.70 (td, J = 1.5, 8.0 Hz, 3H), 7.62 (d, J = 5.1 Hz, 3H), 7.31 (dd, J = 4.7, 8.5 Hz, 3H), 7.13 (dd, J = 2.0, 8.0 Hz, 3H), 7.03 (d, J = 7.8 Hz, 3H), 6.98 (d, J = 6,4 Hz, 3H) ppm. ESI-MS: m/z Calcd. for $C_{48}H_{34}IrN_6$ [M^+]: 885.2445, Found: 885.2439. Anal. Calcd. for $C_{48}H_{33}IrN_6{\cdot}H_2O{\cdot}1.5\ CH_2Cl_2$: C, 57.64; H, 3.71; N, 8.15. Found: C, 57.83; H, 3.68; N, 8.03.

*fac-Tris[2-(5′-(p-pyridyl)phenyl)pyrimidine]iridium(III) (**7**).* *N*-iodosuccinimide (1.49 g, 6.08 mmol) was added to a solution of **9**[22] (100 mg, 152 μmol) in distilled MeCN (25 mL) in the dark. The reaction mixture was stirred at the reflux temperature for 44 h and concentrated under reduced pressure. The resulting residue was dissolved in CH_2Cl_2, and the solution was washed with H_2O. The organic layer was dried over Na_2SO_4, filtered, and concentrated under reduced pressure. The resulting residue was purified by silica gel column chromatography ($CHCl_3$) to afford **11** as a yellow solid (102 mg, 65% yield); mp >300 °C. IR (ATR): ν = 2923, 1719, 1579, 1553, 1451, 1429, 1384, 1255, 1187, 1135, 1064, 1030, 1012, 801 cm^{-1}. ^1H NMR (300 MHz, $CDCl_3$/TMS): δ = 8.73 (dd, J = 2.4, 4.8 Hz, 3H), 8.40 (d, J = 1.8 Hz, 3H), 7.72 (dd, J = 2.4, 8.1 Hz, 3H), 7.19 (dd, J = 2.1, 8.1 Hz, 3H), 6.98 (t, J = 5.4 Hz, 3H), 6.54 (d, J = 8.1 Hz, 3H) ppm. ESI-MS: m/z Calcd. for $C_{48}H_{34}IrN_6$ [M^+]: 1033.8327, Found: 1033.8339.

A mixture of compound **11** (10.0 mg, 9.66 μmol), distilled DMF (1.0 mL), H_2O (0.25 mL), 4-pyridine-boronic acid (7.12 mg, 57.9 μmol), Cs_2CO_3 (18.9 mg, 57.9 μmol), and $PdCl_2(PPh_3)_2$ (1.36 mg, 1.93 μmol) was added to a 10 mL microwave vial, and the solution was degassed by bubbling argon gas through the solution for 15 minutes. The reactor was subjected to microwaving at 120 °C for 30 min. After cooling to room temperature, H_2O (10 mL) and a few drops of 10 N NaOH aq. were added. The organic layer was extracted with $CHCl_3$ (30 mL four times), dried over Na_2SO_4 and concentrated under reduced pressure. The resulting residue was purified by silica gel column chromatography ($CHCl_3$/MeOH = 30:1), and the resulting material was recrystallized from CH_2Cl_2/hexane to afford 7 as a yellow powder (1.98 mg, 23% yield); mp >300 °C. IR (ATR): ν = 3036, 1717, 1590, 1576, 1557, 1445, 1390, 1259, 1187, 1066, 1025, 816, 803, 728 cm^{-1}. ^1H NMR (300 MHz, $CDCl_3$/TMS): δ = 8.80 (dd, J = 2.4, 4.4 Hz, 3H), 8.60 (d, J = 5.7 Hz, 6H), 8.49 (d, J = 1.8, 3H), 7.86 (dd, J = 1.5, 6.0 Hz, 3H), 7.59 (d, J = 6.0 Hz, 6H), 7.31 (dd, J = 1.5, 8.1 Hz, 3H), 7.05 (t, J = 5.7 Hz, 3H), 7.01 (d, J = 8.1 Hz, 3H) ppm. ESI-MS: m/z Calcd. for $C_{48}H_{34}IrN_6$ [M^+]: 888.2303, Found: 888.2298. Anal. Calcd. for $C_{45}H_{30}IrN_9{\cdot}CH_2Cl_2$: C, 56.73: H, 3.31; N, 12.94. Found: C, 56.54; H, 3.44; N, 13.19.

*fac-Tris[2-(5′-(m-pyridyl)phenyl)pyrimidine]iridium(III) (**8**).* Compound **11** was obtained according to the synthesis of **7**. A mixture of compound **11** (20.8 mg, 20.1 μmol), distilled DMF (6.0 mL), H_2O (0.4 mL), 3-pyridine-boronic acid (15.7 mg, 128 μmol), argon-saturated aqueous 2 M KF (0.6 mL), and $PdCl_2$(dppf) (10.5 mg, 60 mol %) was added to a 10 mL microwave vial. Then, the reactor was subjected to microwave irradiation at 120 °C for 45 min. After cooling to room temperature, H_2O (10 mL), a few drops of 10 N NaOH aq. were then added. The organic layer was extracted with $CHCl_3$ (30 mL four times), dried over Na_2SO_4, and concentrated under reduced pressure. The resulting residue was purified by silica gel column chromatography (CH_2Cl_2 to CH_2Cl_2/MeOH = 20:1) and recrystallized from CH_2Cl_2/EtOH/hexane to afford **8** as a yellow powder (4.3 mg, 24% yield); mp >300 °C. IR (ATR): ν = 3365, 1594, 1576, 1558, 1449, 1409, 1382, 1258, 1188, 1070, 1033, 801, 711 cm^{-1}. ^1H NMR (300 MHz, $CDCl_3$/TMS): δ = 8.93 (d, J = 1.2 Hz, 3H), 8.80 (dd, J = 1.8, 3.5 Hz, 3H), 8.53 (dd, J = 1.2, 3.6 Hz, 3H), 8.42 (d, J = 1.8 Hz, 3H), 8.05 (d, J = 5.7 Hz, 3H), 7.87 (dd, J = 1.8, 4.1 Hz, 3H), 7.41 (dd, J = 3.15, 3.9 Hz, 3H), 7.23 (d, J = 1.8 Hz, 3H), 7.03 (m, 6H) ppm. ESI-MS: m/z Calcd. for $C_{48}H_{34}IrN_6$ [M^+]: 888.2303, Found: 888.2293. Anal. Calcd. for $C_{45}H_{30}IrN_9{\cdot}2CH_2Cl_2$: C, 53.31; H, 3.24; N, 11.91. Found: C, 53.28; H, 3.43; N, 11.69.

Measurements of UV/vis Absorption and Luminescence Spectra. UV/vis spectra were recorded on a JASCO V-550 UV/vis spectrophotometer and emission spectra were recorded on a JASCO FP-6200 spectrofluorometer at 298 and 77 K. Sample solutions in quartz cuvettes equipped with Teflon septum screw caps were degassed by bubbling Ar through the solution for 10 min prior to luminescence measurements. The quantum yields for luminescence (Φ) were determined by comparison with the integrated corrected emission spectrum of a quinine sulfate standard, whose emission quantum yield in 0.1 M H_2SO_4 was assumed to be 0.55 (excitation at 366 nm). Equation 1 was used in calculating the emission quantum yields, in which Φ_s and Φ_r denote the quantum yields of the sample and reference compound, η_s and η_r are the refractive indexes of the solvents used for the measurements of the sample and reference (1.477 for dimethylsulfoxide (DMSO) (η_s) and 1.333 for H_2O (η_r)), A_s and A_r are the absorbance of the sample and the reference, and I_s and I_r stand for the integrated areas under the emission spectra of the sample and reference, respectively (all of the Ir compounds were excited at 366 nm for luminescence measurements in this study). For the determination of Φ_s in mixed-solvent systems, the η values of the main solvents were used for the calculation.

$$\Phi_s = \Phi_r(\eta_s^2 A_r I_s)/(\eta_r^2 A_s I_r) \quad (1)$$

The luminescence lifetimes of sample solutions in degassed DMSO at 298 K were measured on a TSP1000-M-PL (Unisoku, Osaka, Japan) instrument by using THG (355 nm) of Nd: YAG laser, Minilite I (Continuum, CA, U.S.A.) as excitation source. The signals were monitored with an R2949 photomultiplier. Data were analyzed by using the nonlinear least-squares procedure.

UV/vis Absorption Spectral Change of DPBF. The solutions of Ir complexes (12 μM) in DMSO/H_2O (1.3/1.2, v/v) (2.5 mL) were aerated for 10 min, to which a solution of 1,3-diphenylisobenzofuran (DPBF, 300 μM) in DMSO (500 μL) was added. The resulting solutions containing 10 μM Ir complex and 50 μM DPBF in DMSO/H_2O (3/2) were photoirradiated at 366 nm at 25 °C and changes in the UV/vis spectra of DPBF were recorded.

ESR Analysis of Nitroxide Radicals Generated by the Reaction of TPC with Singlet Oxygen.[23] Solutions of Ir complexes (40 μM) and 2,2,5,5-tetramethyl-3-pyrroline-3-carboxamide (TPC) (80 mM) in DMSO/H_2O (3/2, v/v) (200 μL) were prepared, and the

dx.doi.org/10.1021/ic402387b | Inorg. Chem. 2014, 53, 409−422

resulting solutions were then photoirradiated at 365 nm (Twinlight365 (RELYON)) at 25 °C. After the photoirradiation, the samples were transferred to a quartz cell, and electron spin resonance (ESR) spectra were recorded on an X-band ESR spectrometer (JES-FA-100, JEOL, Tokyo, Japan). The conditions used for the ESR measurements were as follows: field sweep, 330.50−340.50 mT; field modulation frequency, 100 kHz; field modulation width, 0.05 mT; amplitude, 80; sweep time, 2 min; time constant, 0.03 s; microwave frequency, 9.420 GHz; microwave power, 4 mW. To calculate the spin concentration of each nitroxide radical, 20 μM 4-hydroxy-2,2,6,6-tetramethylpiperidine *N*-oxyl (TEMPOL) was used as a standard sample, and the ESR spectrum of manganese (Mn^{2+}) which was located in the ESR cavity was used as an internal standard. The spin concentration was determined using Digital Data Processing (JEOL, Tokyo, Japan).

Photooxidation of Thioanisole. The solutions of **5** or **6** (11 μM) and NaN_3 (110 mM) in DMSO-*d6*/D_2O (350/280, v/v) (630 μL) were aerated for 10 min, to which a solution of thioanisole (100 mM) in DMSO-*d6* (70 μL) was added. The resulting solutions containing 10 μM Ir complex (**5** or **6**) and 10 mM thioanisole in DMSO-*d6*/D_2O (3/2) were photoirradiated at 365 nm (Twinlight365 (RELYON)) at 25 °C, and changes in the ^1H NMR (400 MHz) spectra of thioanisole were recorded.

Cell Cultures and Luminescence Imaging.[12] HeLa-S3 cells, which were provided by Dr. Tomoko Okada (National Institute of Advanced Industrial Science and Technology), were grown in MEM supplemented with 10% FCS (fetal calf serum) under 5% CO_2 at 37 °C. HeLa-S3 cells (2.0×10^5 cells/mL) were plated in 1.0 mL of MEM on 24 well plates (Nunclon) under the same conditions and allowed to adhere for 24 h. Subsequently, when 0.5 mL of MEM was removed, 0.5 mL of MEM containing **5** (20 μM) in MEM/DMSO (49/1) was added, and the samples in MEM/DMSO (99/1, v/v) were incubated at 37 °C under 5% CO_2 for 30 min. The culture medium was then removed and washed twice with PBS (phosphate buffered saline). Finally, 2.0 mL of MEM was added for luminescence imaging by fluorescence microscopy of the Ir complexes with excitation at 377 nm (FF01 filter (377 ± 50) nm was used for excitation to obtain emission images from Ir complexes). Costaining with 10 μM **5** and 10 nM MitoTracker, and 10 μM **5** and 100 nM LysoTracker was carried out with excitation at 540 nm for MitoTracker and LysoTracker.

Photoinduced Cell Death and PI Staining. HeLa-S3 cells were incubated in MEM/DMSO (99/1, v/v) containing a given Ir complex (10 μM) for 30 min at 37 °C, and washed twice with PBS. Then, 0.5 mL of MEM was added, and the solution subjected to photoirradiation at 465 nm (Twinlight465 (RELYON, Japan)) for 10 min at 25 °C. Subsequently, 3.0 μL of PI solution (1 mM) was added, and the solution was incubated for 1 h at 37 °C. The culture medium was then removed and washed twice with PBS. Finally, 100 μL of MEM was added for observation (excitation at 540 nm for PI) on a BIOREVO BZ-9000 instrument (Keyence, Japan).

Inductively Coupled Plasma−Atomic Emission Spectrometry (ICP-AES) Experiments.[12] HeLa-S3 cells were incubated in 100 mm-coating dishes under an atmosphere of 5% CO_2 at 37 °C for 72 h. The culture medium was removed, and the cells were washed gently with PBS (5 mL). The cell layer was then was trypsinized under an atmosphere of 5% CO_2 at 37 °C. The numbers of HeLa-S3 cells were counted (ca. 1.0×10^7 cells), and these cells were incubated in MEM/DMSO (99/1, v/v) with **1** (10 μM), **4** (10 μM), and **5** (10 μM), respectively, under an atmosphere of 5% CO_2 at 37 °C for 30 min. The culture medium and trypsinized medium solution were transferred into 50 mL centrifuge tubes and centrifuged at 4 °C (1400 rpm for 7 min). The medium was removed, and HeLa-S3 cells were transferred to a 15 mL centrifuge tube with MEM (5 mL × 2). After centrifugation at 1400 rpm and 4 °C for 7 min, the medium solution was removed. After transferring the HeLa-S3 cells to a 1.5 mL eppendorf tube with MEM (0.45 mL × 2), they were centrifuged at 2000 rpm and 4 °C for 10 min and the medium solution was removed. RIPA (Radio-Immunoprecipitation Assay) buffers (500 μL) were then added and the sample was allowed to stand in the centrifuge tubes at 0 °C for 30 min. The solution in these centrifuge tube was centrifuged at 15000 rpm and 4 °C for 10 min, and the supernatant liquid (400 μL) (portion A) was taken and diluted with 5% HCl aq. (6 mL) and moved to the other vial (portion B). To the remaining material in the centrifuge tube after taking portion B, 1 mL of 1 M HCl aq. was added, vortexed, and incubated at 37 °C for 24 h. The resulting mixture was centrifuged at 15000 rpm and 4 °C for 10 min, and the supernatant, 1 mL of the resulting sample (portion C) was taken (1 mL) and mixed with portion B (this process was repeated again). The volume of the mixture of portion B and C was made up to 10 mL and then centrifugated at 3000 rpm and 4 °C for 10 min for ICP-AES analysis on Shimadzu ICPE-9000.

RESULTS AND DISCUSSION

Design of Ir(4Pyppy)$_3$ 5 and Ir(3Pyppy)$_3$ 6 Based on DFT Calculations. First, DFT calculations were carried out for **5**, H_3·**5**, **6**, and H_3·**6** using the Gaussian03 program (B3LYP, LanL2DZ basis set for the Ir atom, and the 6-31G basis sets for the H, C, N atoms) to predict their emission properties.[15] The HOMO and LUMO energies were obtained by single point calculations of the optimized Ir complexes.

We previously reported that the protonation of the three amino groups of Ir(III) complexes **3** and **4** at an acidic pH results in an increase in the HOMO−LUMO energy gap (Figure 1a), resulting in a blue-shift in the emission wavelength.[8,12,16] In contrast, the protonation of nitrogen atoms on the pyridine rings of **5** and **6** resulted in a decrease in the HOMO−LUMO energy gap (Figure 1b and 1c). Therefore, it was predicted that **5** and **6** would exhibit different pH-dependent photochemical properties (i.e., a red-shift in the emission wavelength) from those of **3** and **4**. The results of similar DFT calculations for **7** and **8** suggested that their behavior would be similar to that for **5** and **6** (Supporting Information, Figure S1).

Synthesis of Ir(4Pyppy)$_3$ 5, Ir(3Pyppy)$_3$ 6, Ir(4Pyppym)$_3$ 7, Ir(3Pyppym)$_3$ 8. For the synthesis of **5** and **6**, **1** was treated with *N*-iodosuccinimide in CH_2Cl_2 to give **10** in 55% yield.[8] The Suzuki−Miyaura cross-coupling reaction[20] of **10** with 4-pyridine-boronic acid in the presence of $PdCl_2(PPh_3)_2$ and Cs_2CO_3 in freshly distilled DMF at 120 °C gave **5** in 42% yield (Chart 4). Complex **6** was obtained from **10** with 3-pyridine-boronic acid in the presence of $PdCl_2$(dppf) and KF[21] in DMF at 120 °C in 47% yield. The *fac*-Ir(ppym)$_3$ **9**[22] was next treated with NIS in MeCN to give **11** and converted to **7** and **8**. The Suzuki−Miyaura cross-coupling reaction of **11** with 4-pyridine-boronic acid in the presence of $PdCl_2(PPh_3)_2$ and Cs_2CO_3 in freshly distilled DMF at 120 °C gave **7** (15% yield for 2 steps from **9**) (Chart 4). The complex **8** was obtained from **11** by reaction with 3-pyridine-boronic acid in 16% yield from **9**.

Photochemical Properties of Ir(4Pyppy)$_3$ 5 and Ir(3Pyppy)$_3$ 6. Figure 2a presents the UV/vis absorption spectra of **5** in DMSO, in which acid-free **5** (10 μM) exhibits strong absorption maxima at 291 and 340 nm and the addition of hydrochloric acid in 1,4-dioxane caused a substantial red-shift (ca. 57 nm). In the case of **6** (10 μM), acid-free **6** (10 μM) had absorption maxima at 289 and 325 nm, and exhibited a slight red-shift (ca. 16 nm) with a small color change upon acidification (Figure 2b). The UV/vis spectra of Ir complexes **7** and **8** were similar to those of **5** and **6**, respectively (Supporting Information, Figure S2).

The luminescence of **5** in degassed DMSO exhibited an emission maximum at about 506 nm as shown in Figure 3a. The addition of H^+ to **5** induced a significant red-shift (ca. 100 nm) in its luminescence emission, resulting in a red-colored

dx.doi.org/10.1021/ic402387b | *Inorg. Chem.* 2014, 53, 409−422

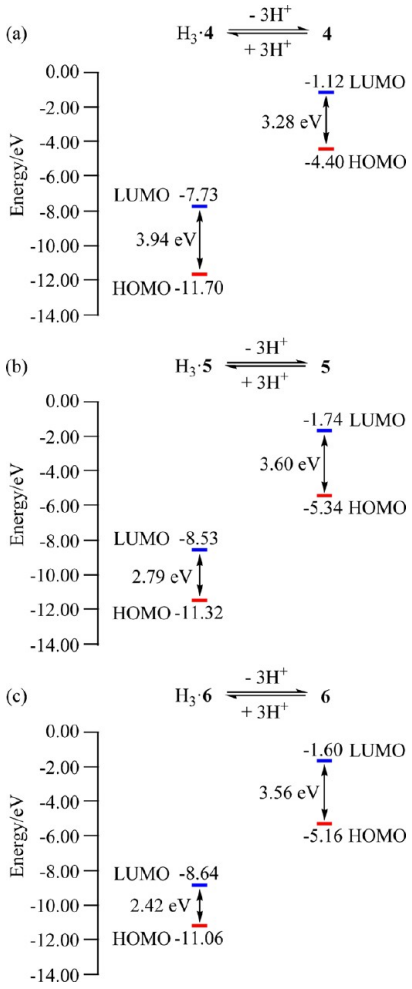

Figure 1. HOMO and LUMO energy of Ir(III) complexes, **4**–**6**, and their energy gap calculated by the Gaussian03 program using the B3LYP hybrid functional together with the LanL2DZ basis for the Ir atom and the 6-31G basis sets for the H, C, N atoms. (a) Ir(deatpy)$_3$ **4** and H$_3$·**4**, (b) Ir(4Pyppy)$_3$ **5** and H$_3$·**5**, and (c) Ir(3Pyppy)$_3$ **6** and H$_3$·**6**.

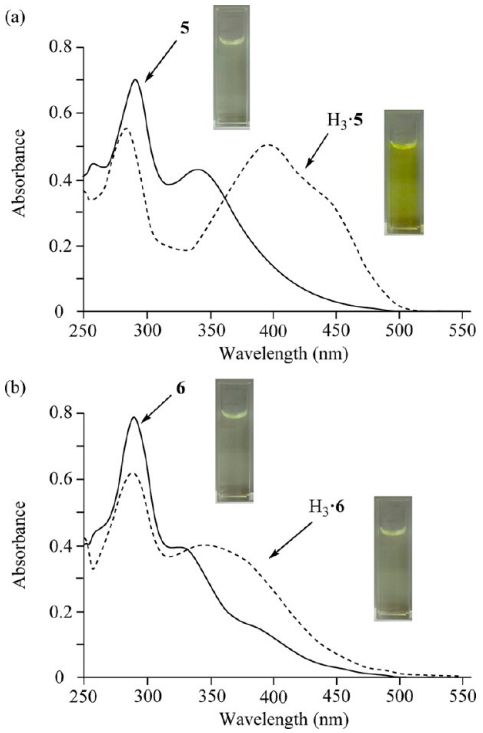

Figure 2. UV/vis spectra of (a) **5** (10 μM) and (b) **6** (10 μM) in degassed DMSO at 298 K before and after the addition of HCl in 1,4-dioxane.

emission at 593 nm upon protonation of the pyridyl groups. When a base, 1,8-diazabicyclo[5.4.0]undec-7-ene (DBU), was added, the green color emission was recovered, and a reversible change in the emission intensity and wavelength was observed by the repeated addition of an acid or a base. In contrast, acid-free **4** exhibited a weak emission at about 550 nm, and acidification induced a significant blue-shift (ca. 60 nm) with an enhancement in the green-colored emission at 497 nm (Figure 3b). This contrary emission behavior of **4** (dashed curve) and **5** (plain curve) is clearly displayed in Figure 3c.

Chart 4

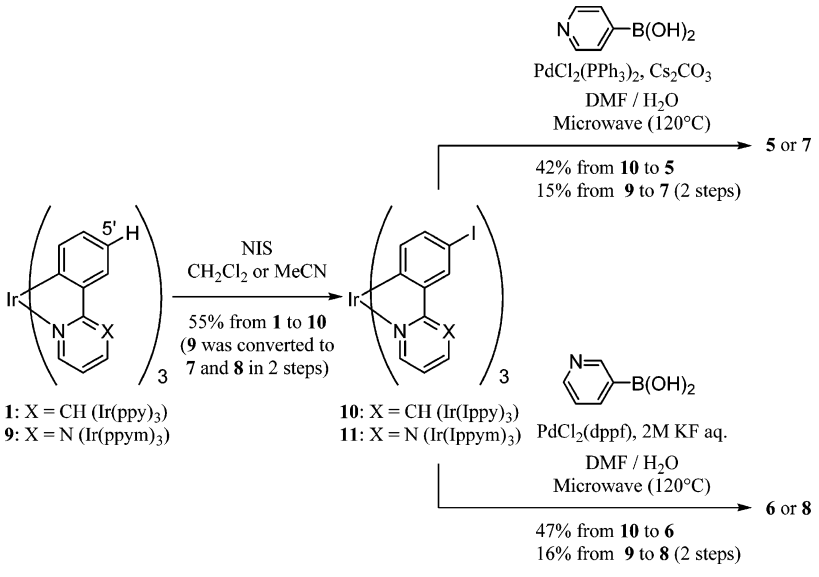

dx.doi.org/10.1021/ic402387b | Inorg. Chem. 2014, 53, 409–422

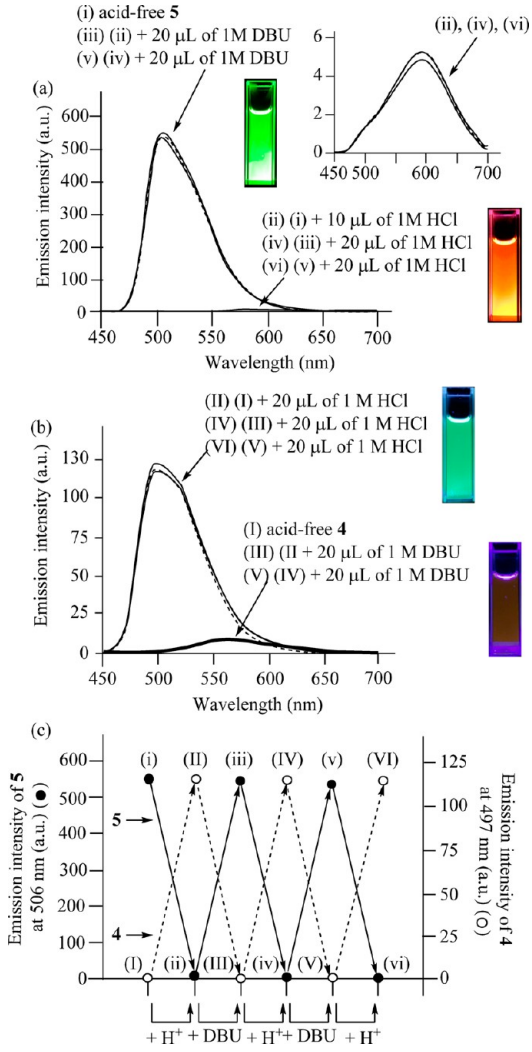

Figure 3. (a) Change in luminescence emission spectra of **5** (10 μM) in degassed DMSO at 298 K (excitation at 366 nm) upon the repeated addition of an acid (1 M HCl in 1,4-dioxane) and a base (1 M DBU in 1,4-dioxane). (i) acid-free **5**, (ii) (i) + HCl, (iii) (ii) + DBU, (iv) (iii) + HCl, (v) (iv) + DBU, and (vi) (v) + HCl. (Inset of Figure 3a) Expansion of the emission spectrum of H_3·**5** (ii, iv, and vi). (b) Change in luminescence emission spectra of **4** (10 μM) in degassed DMSO at 298 K (excitation at 366 nm) upon the repeated addition of acid (1 M HCl in 1,4-dioxane) and base (1 M DBU in 1,4-dioxane). (I) acid-free **4**, (II) (I) + HCl, (III) (II) + DBU, (IV) (III) + HCl, (V) (IV) + DBU, and (VI) (V) + HCl. (c) Change in emission intensity of **5** at 506 nm (plain curve) and **4** at 497 nm (dashed curve) caused by the repeated addition of HCl and DBU. A.u. is in arbitrary units.

Acid-free **6** exhibited a green-colored emission at around 513 nm in degassed DMSO, the wavelength of which is slightly longer than that of **5**, as shown in Supporting Information, Figure S3. The repeated addition of H^+ and DBU to **6** induced a change in the emission spectra that was similar to that of **5**. The quantum yields (ϕ) of these complexes in DMSO are summarized in Table 1.

The luminescence behavior of complex **7** and **8**, which contain 2-phenylpyrimidine (ppym) ligands, is similar to that of complex **5** and **6**, respectively. The luminescence of **7** in degassed DMSO exhibited an emission maximum at about 512 nm and a yellow-green-colored emission (Supporting Information, Figure S4a and Table 1). Acidification induced a significant red-shift (ca. 50 nm) and the orange-colored

Table 1. Photophysical Properties of 5, 6, 7, and 8 in Degassed DMSO at 298 K[a]

complex	λ_{max}(absorption)	λ_{max}(emission)	Φ_{PL}	$\tau(\mu s)$
5	258 nm, 291 nm, 340 nm	506 nm	0.57	1.26
H_3·**5**	284 nm, 397 nm	593 nm	8.1×10^{-3}	0.39
6	289 nm, 325 nm	513 nm	0.57	1.35
H_3·**6**	288 nm, 341 nm	513 nm	2.5×10^{-3}	0.53
7	280 nm, 331 nm	512 nm	0.46	1.38
H_3·**7**	276 nm, 382 nm	562 nm	3.1×10^{-2}	0.79
8	276 nm, 320 nm	519 nm	0.32	1.38
H_3·**8**	279 nm, 327 nm	519 nm	2.9×10^{-3}	0.69

[a]1M HCl/1,4-dioxane was used for complete protonation.

emission at around 562 nm.[24] As shown in Supporting Information, Figure S4b, the acid-free form and the protonated form of complex **8** exhibited a green-colored emission at around 519 nm. Protonation of three pyridyl groups induced a substantial decrease in emission intensity at 519 nm without any significant change in the emission wavelength.

Luminescence spectra and photos of **5** (10 μM) and **6** (10 μM) in degassed DMSO/100 mM buffer (from pH 4 to 10) (1/6) at 298 K are shown in Figures 4 and 5.[25] Complex **5** exhibited a weak red-orange emission at acidic pH (600 nm at pH 4−5, 560 nm at pH 6). The emission intensity of **5** and **6** at 498 or 509 nm were dramatically increased at > pH 6, and a strong green emission was observed at basic pH (498 nm at pH 8−10), as plotted in Figure 4c and 4d, respectively. No red-shift in the emission wavelength was observed for **6**, and emission at pH 4 was very weak.

Complex **7** exhibited a weak orange-colored emission at acidic pH (559 nm at pH 4−5, 543 nm at pH 6 (Supporting Information, Figure S7)).[26] The emission intensity at 523 nm was substantially increased at pH 6−7, and a strong yellow emission was observed at basic pH (523 nm at pH 8−10). Unfortunately, it was not possible to obtain pH-dependent emission spectra of complex **8**, because the solubility of **8** is low and its luminescence is very weak, even at a concentration of 1 μM.

The pK_a values of H_3·**5** in the ground state were estimated to be below 6 from a plot of the relative absorbance at 330 nm (closed square) in Supporting Information, Figure S9a, and those in the excited state were estimated to be approximately in the range of 5 to 9 from the curve of the emission intensity (open circle) in Supporting Information, Figure S9a, implying that the pK_a values for this compound in the ground state and excited state are significantly different. In our previous research, the pK_a values of Ir complexes **3** and **4** were found to be nearly the same in the ground and excited state.[8,12] Complex **5** is our first compound with different pK_a values between the ground state and excited state. This point will be discussed below in more detail. From Supporting Information, Figure S9b, it is likely that properties of **6** would be similar.

The approximate pK_a values of H_3·**7** in the ground state appear to be in the range of 4 to 6, based in Supporting Information, Figure S8, and the corresponding values for the excited state were estimated to be in the range of 5 to 8, which are slightly lower than those of **5** (Supporting Information, Figure S7b). The lower pK_a values of H_3·**7** than H_3·**5** might be attributable to the electron-withdrawing effect of the ppym ligand.

Based on the DFT calculations regarding **5** and **6** (Figure 6), the HOMO of these complexes are located on the phenyl π and

dx.doi.org/10.1021/ic402387b | Inorg. Chem. 2014, 53, 409−422

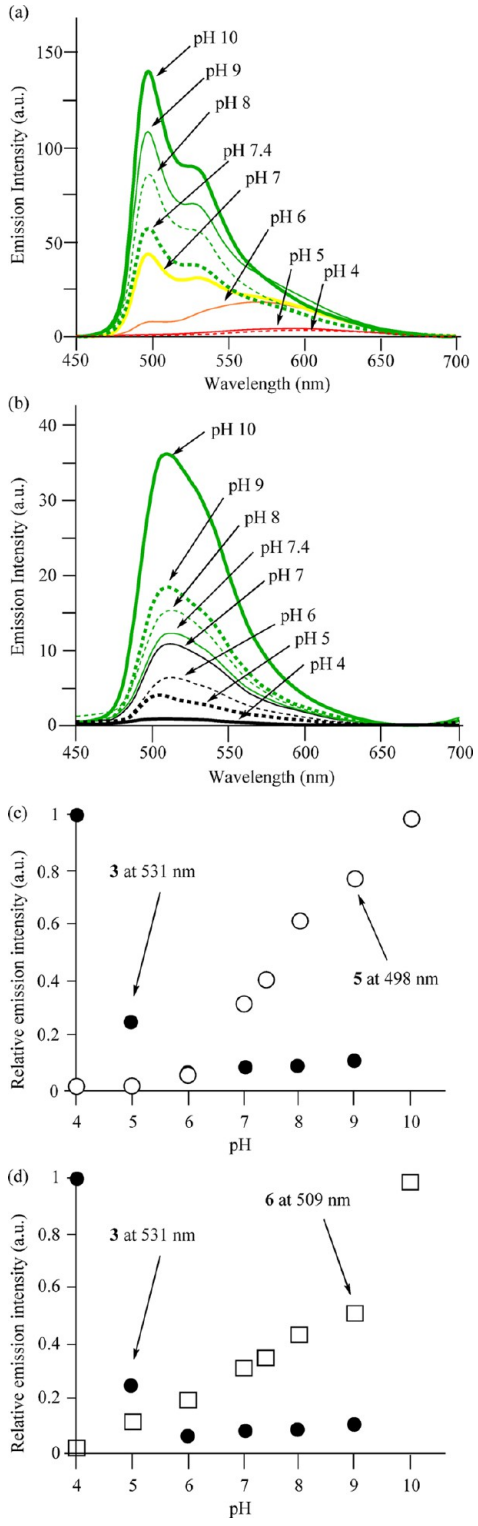

Figure 4. (a), (b) Change in the emission spectra of (a) **5** or (b) **6** (10 μM) in degassed DMSO/100 mM buffer (from pH 4 to 10) (1/6) at 298 K. (c), (d) pH-Dependent emission intensity of (c) **5** (10 μM) at 498 nm (open circles) and (d) **6** (10 μM) at 509 nm (open squares) and that of **3** (10 μM) at 531 nm (closed circles). The relative emission intensities of **5** and **6** were calculated based on **1** at pH 10, and that of **3** was calculated based on **1** at pH 4. Excitation at 366 nm. A.u. is in arbitrary units.

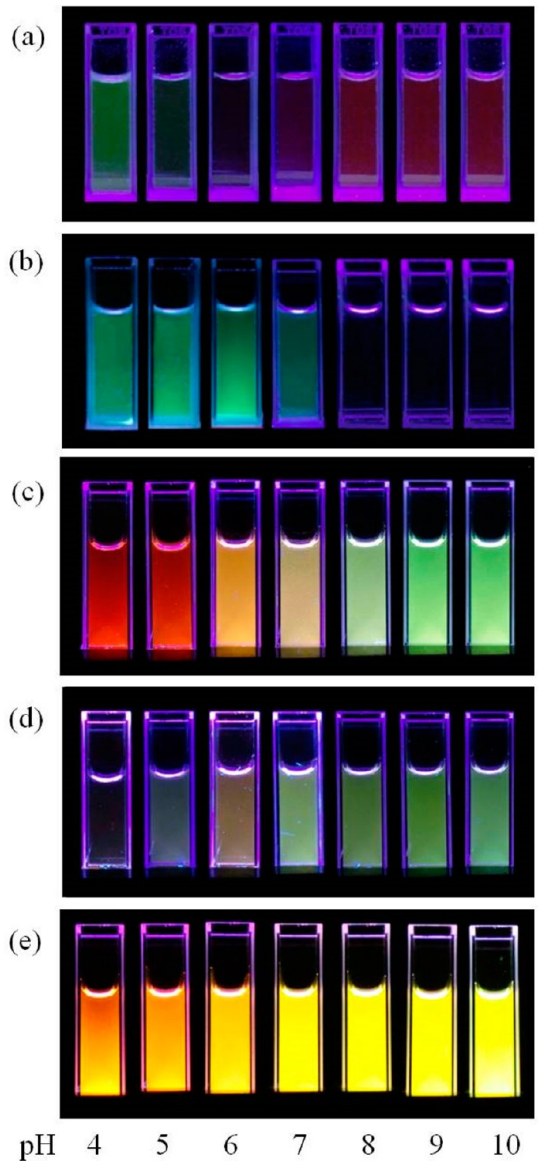

Figure 5. Photograph showing solutions of (a) **3** (100 μM), (b) **4** (1 μM), (c) **5** (10 μM), (d) **6** (10 μM), and (e) **7** (10 μM) in degassed DMSO/100 mM buffer (from pH 4 to 10) (1/6) at 298 K. Excitation at 366 nm.

Ir d orbitals and the LUMO is mainly located on the pyridine rings on the ppy ligands, which is indicative of metal-to-ligand charge-transfer (MLCT) and ligand-centered (LC) transitions.[27] While the HOMOs for H_3·**5** and H_3·**6** are similar to those of **5** and **6**, their LUMOs are mainly localized on the protonated pyridine rings. These results indicate the occurrence of new lower-lying MLCT transitions from the phenyl π and d orbitals of Ir to protonated pyridine rings and an intraligand charge-transfer (ILCT) transition between the ppy ligand and protonated pyridine ring,[16] resulting in a significant red-shift in the UV−vis spectra of H_3·**5** and H_3·**6**. The DFT calculations for **7** and **8** indicated that the locations of the HOMO and the LUMO were similar to those of **5** and **6**, respectively (Supporting Information, Figure S10).

The LUMO for H_3·**5** is mainly located on the protonated pyridine rings, and the MLCT process might result in the protonated pyridine rings being more electron-rich than in the ground state (Figure 6a, left).[28] Therefore, the protonated form of **5** in the excited state would be expected to be more stabilized than that in the ground state, which may account for

dx.doi.org/10.1021/ic402387b | *Inorg. Chem.* 2014, 53, 409−422

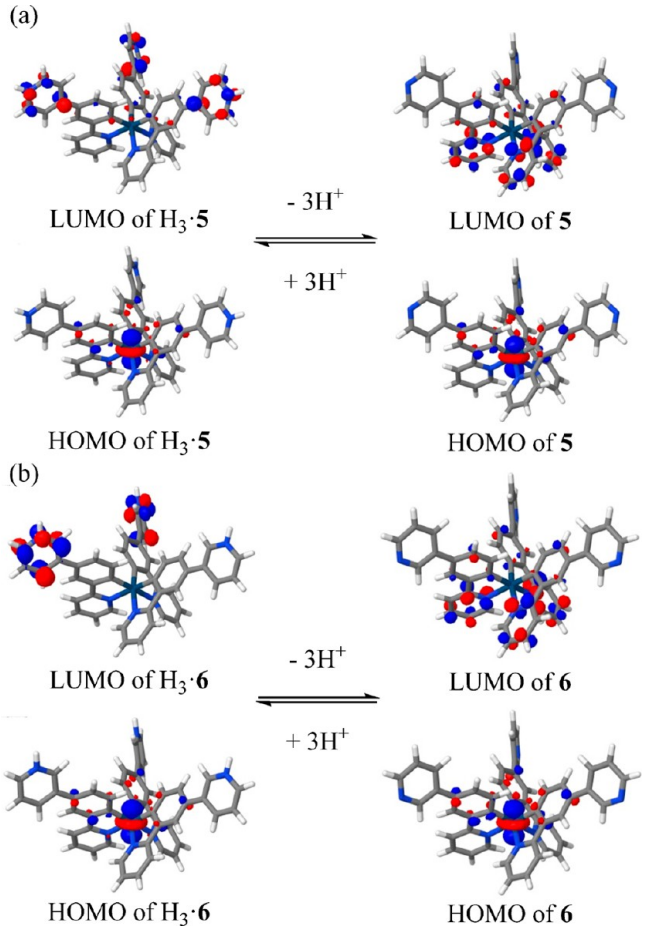

Figure 6. HOMO and the LUMO surface of Ir(III) complexes, **5** and H_3·**5** (a), and **6** and H_3·**6** (b) calculated by the Gaussian03 program using the B3LYP hybrid functional together with the LanL2DZ basis for the Ir atom and the 6-31G basis sets for the H, C, and N atoms.

the higher pK_a value of **5** in the excited state compared to that in the ground state.

The TD-DFT calculation results were examined in more detail, in an attempt to better understand the aforementioned luminescence behaviors of **5**, **6** and their protonated forms (Supporting Information,Table S1). The excitation energies for triplet states of acid-free **5** and **6** were estimated to be 2.6 eV/ca. 475 nm, which can be assigned to ^{3}MLCT (from the phenyl π and Ir d orbitals to the pyridine rings directly bound to Ir) and ^{3}LC (ppy ligands) transitions (Supporting Information,Table S1). Their calculated emission wavelengths were in good agreement with the experimental results as shown in Figure 3 and Table 1 (Em 506 nm for **5**, Em 513 nm for **6**). The TD-DFT calculation for H_3·**5** suggested its emission at about 593 nm originated from a new lower-lying ^{3}MLCT transition (from the phenyl π and Ir d orbitals to the protonated pyridine rings) and/or probably ^{3}ILCT transitions (between ppy ligands and the protonated pyridine rings). The calculated excitation energies for H_3·**5** of about 2.1 eV (ca. 600 nm) are in agreement with the observed emission at 593 nm (Table 1). Although the TD-DFT results for H_3·**6** also show a significant red-shift in the emission wavelength, similar to that of H_3·**5**, the protonation of **6** induced only a negligible change in the emission wavelength. We assume that the red emission of H_3·**6** at about 675 nm was quenched by an additional nonradiative deactivation process induced by protonation, resulting in an emission only from the emissive state, similar to that of acid-free **6**.

The emission spectra of **5** and **6** at 77 K (Supporting Information, Figure S11) were similar to that of complex **1**,[1h] indicating that the phosphorescence exhibited by these complexes arose mainly from the ^{3}MLCT (from Ir to ppy ligand) excited state and that the effect of the three pyridyl groups of the acid-free complexes **5** and **6** is negligible. The red-shift of a solution of **5** as the result of the protonation of the three pyridyl rings is smaller at 77 K (from 488 to 537 nm, 49 nm) than that at room temperature (at 506 to 593 nm, 87 nm). Interestingly, the luminescence of **6** exhibited a red-shift due to the protonation at 77 K, although a negligible change was observed at room temperature. It is likely that the luminescence of **5** and **6** at 77 K is due to alternate transition states that are deactivated at room temperature.

Generation of Singlet Oxygen by the Photoirradiation of Ir Complexes. Some groups reported that Ir(III) complexes can function as efficient sensitizers and can activate triplet oxygen to singlet oxygen ($^1O_2$) and their applications to photooxidation reactions.[13,29] In a previous study, we reported

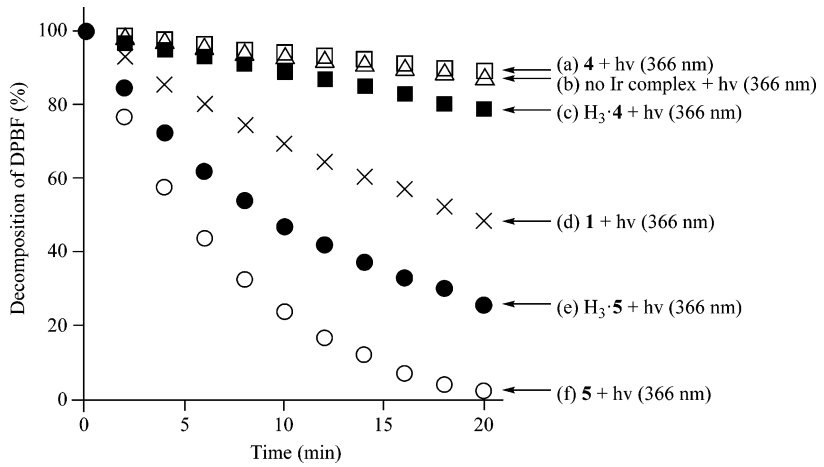

Figure 7. Comparative photooxidation of 1,3-diphenylisobenzofuran (DPBF) (50 μM) in DMSO/H_2O (3/2) at 298 K, (a) **4** (open squares), (b) blank (open triangle), (c) H_3·**4** (closed squares), (d) **1** (cross), (e) H_3·**5** (closed circles), (f) **5** (open circles) (excitation at 366 nm). [Ir complexes] = 10 μM.

dx.doi.org/10.1021/ic402387b | Inorg. Chem. 2014, 53, 409−422

on the pH-dependent generation of $^1O_2$ by the photoirradiation of **4** and role in the necrosis-like cell death of HeLa-S3 cells.[12] These results allowed us to verify that $^1O_2$ is generated by **5** and **6**. The oxidation of a sulfide to a sulfoxide or sulfone is one of the representative photooxidation reactions with $^1O_2$.[30] We followed the oxidation of thioanisole by the photoirradiation of Ir complexes by ^1H NMR (400 MHz), as shown in Supporting Information, Figure S12 and S13, which clearly indicate that these Ir complexes function as catalysts of the photochemical oxidation of thioanisole.[31] The presence of NaN_3, the specific quencher of $^1O_2$,[32] essentially inhibited this photooxidation reaction, thus probing the formation of $^1O_2$ in the reaction mixture.

The decomposition of 1,3-diphenylisobenzofuran (DPBF) was also monitored by UV/vis spectra measurement.[12,33] As shown in Figure 7, the findings show that the photoirradiation of acid-free **5** facilitates the decomposition of DPBF, again, possibly because of the generation of $^1O_2$. Interestingly, $^1O_2$ generation was suppressed when these compounds were protonated, which are different phenomena from that of **4**, whose protonated form (H_3·**4**) produces $^1O_2$ more efficiently than its acid-free form. We presume that these results are indicative of the existence of a correlation between a HOMO−LUMO energy gap and the generation of $^1O_2$.[13b,34] Compared to **5**, complex **6** was somewhat less efficient in generating $^1O_2$ (Supporting Information, Figure S13 and S14). It should also be noted that DPBF was decomposed by complex **5** and **6** faster than **1** and **4**, possibly because of the larger absorbance at 366 nm compared to that for **1** and **4**.

It was considered that the decomposition of DPBF is caused not only by $^1O_2$ but also other reactive oxygen species (ROS).[35] Kohno's group recently reported on the analytical methods for photogenerating $^1O_2$, in which an ESR analysis is used to measure nitroxide radicals that are generated through the oxidation of sterically hindered amines, such as 2,2,6,6-tetramethyl-4-piperidinol (4-hydroxy-TEMP) and 2,2,5,5-tetramethyl-3-pyrroline-3-carboxamide (TPC) (Chart 5).[23]

Chart 5

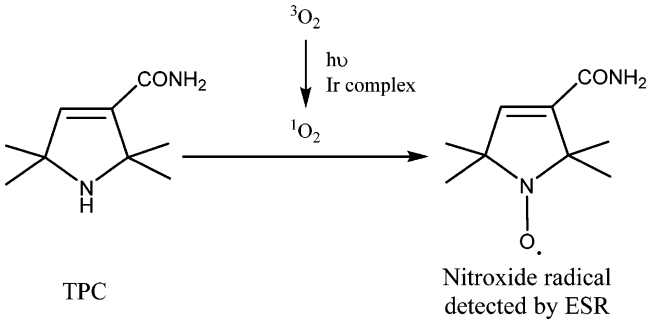

Changes in the ESR signals of nitroxide radical of TPC generated by the photoirradiation of Ir complexes are shown in Supporting Information, Figure S15 and Figure 8, which verify the generation of $^1O_2$.[36]

Live Cell Imaging Using 5 with MitoTracker and LysoTracker Dye. Costaining studies of **1** or **5** with a lysosomal dye (LysoTracker) and a mitochondrial dye (MitoTracker) were conducted (Figure 9), because it is known that the pH of lysosomes is lower than 5.5[12,37] and the pH of mitochondria is about 7.5.[38] After incubating HeLa-S3 cells in MEM/DMSO (pH 7.4, 99/1, v/v) with **1** and **5** (10 μM) for 30 min at 37 °C, the cells were washed with PBS and then, observed by fluorescent microscopy (BIOREVO BZ-9000, Keyence). It is interesting to note that luminescent images were obtained in the presence of **1** and **5** (Figure 9b, 9f, 9j and 9n). The emission of **1** and **5** is delocalized in the cytosol of HeLa-S3 cells, rather than the nucleus. Figure 9a−d displays a typical bright field image (Figure 9a), a luminescent image of **1** (Figure 9b), a luminescent image of LysoTracker (Figure 9c), and a merged image (Figure 9d) of Figure 9b and 9c. It is likely that the area stained by **1** and LysoTracker are partly overlapped. Figure 9e−h shows the results for the costaining of HeLa-S3 cells with **1** and MitoTracker. The merged images of Figures 9d and 9h show yellow regions and wide green regions, indicating that **1** is located in mitocondria and lysosomes in addition to the cytosol.

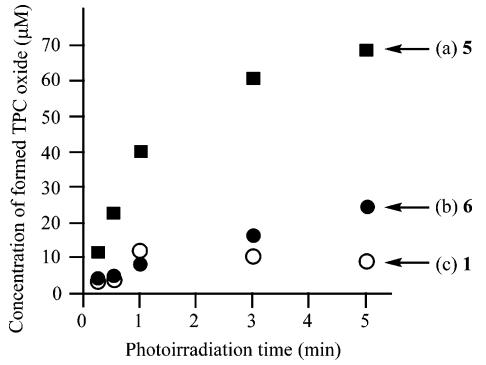

Figure 8. Photooxidation of 2,2,5,5-tetramethyl-3-pyrroline-3-carboxamide (TPC) (80 mM) in DMSO/H_2O (3/2) at 298 K, (a) **5** (closed squares), (b) **6** (closed circles), (c) **1** (open circles). [Ir complexes] = 40 μM.

The typical bright field image, luminescent image with **5** and LysoTracker, and the corresponding merged image (Figure 9i−l) indicate that **5** is weakly overlapped with LysoTracker. On the other hand, the luminescent overlay image (Figure 9p) of **5** (Figure 9n) and MitoTracker (Figure 9o) shows that some yellow regions are present, indicating that **5** and MitoTacker stain the same organelles. These results suggest that the protonated form of **5** exhibits negligible emission in acidic organelles such as lysosomes, and the deprotonated form of **5** emits a green color in neutral to basic organelles such as mitochondria. These results are consistent with the luminescent behavior of **5** in the aqueous solution shown in Figures 4 and 5. The similar cellular uptake behavior of **1** and **5** were observed at 4 °C (Supporting Information, Figure S16), suggesting that these complexes were taken up into the cells by passive transport.

Induction of Cell Death of HeLa-S3 Cells upon Photoirradiation in the Presence of Ir Complexes. We previously reported on the photoinduced cell death of HeLa-S3 cells upon photoirradiation of **4** at 377 nm.[12,39] The findings of this study indicate that cell death is induced in HeLa-S3 cells upon photoirradiation of **5** at 377 and 470 nm. Figure 10 shows timelapse images of HeLa-S3 cells after photoirradiation at 377 and 470 nm for 30 min. After photoirradiation for 20 min, the membranes of the HeLa-S3 cells began to swell, and this swelling continued during the entire period of photoirradiation. On the other hand, negligible membrane swelling was observed by photoirradiation in the absence of **5** or by no photoirradiation in the presence of **5**, clearly suggesting that the swelling of the cell membrane was caused by the photo-

dx.doi.org/10.1021/ic402387b | Inorg. Chem. 2014, 53, 409−422

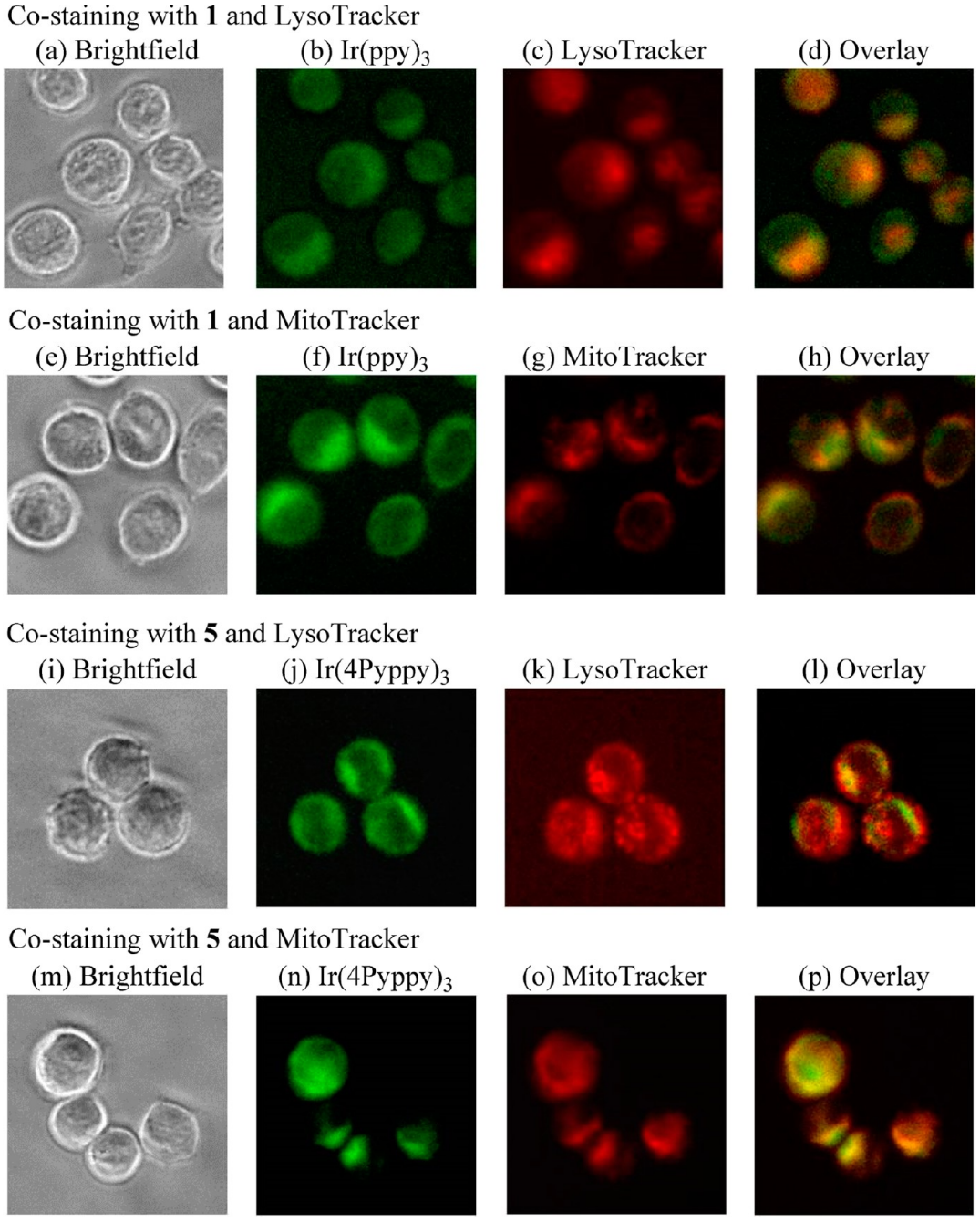

Figure 9. Luminescence microscope images (BIOREVO BZ-9000, Keyence) of HeLa-S3 cells stained with Ir complexes (10 μM) and LysoTracker (100 nM), or MitoTracker (10 nM) in MEM/DMSO (99/1, v/v) at 37 °C for 30 min. (a), (e), (i), and (m) brightfield image of HeLa-S3 cells, (b) and (f) emission images of **1**, (j) and (n) emission images of **5**, (c) and (k) emission images of LysoTracker, (g) and (o) emission images of MitoTracker, (d) overlay image of (b) and (c), (h) overlay image of (f) and (g), (l) overlay image of (j) and (k), (p) overlay image of (n) and (o). Excitation at 377 nm for Ir complexes and excitation at 540 nm for LysoTracker and MitoTracker.

irradiation of **5**, even by irradiation at 465−470 nm, a wavelength that is less toxic than 377 nm light.

In our previous work, we concluded that the photoirradiation of **4** induces necrosis-like cell death of HeLa-S3 cells.[12] It was assumed that H_3·**4** formed in lysosome generates $^1O_2$ more efficiently than its acid-free form to facilitate lysosomal breakdown, resulting in necrosis-like cell death.

We suspected that the type of cell death may be altered by the use of **5** as an O_2 activator. Figure 11a−c show a brightfield image (Figure 11a), a propidium iodide (PI) emission image (Figure 11b), and an overlay image (Figure 11c) after photoirradiation at 465 nm for 10 min in the presence of **5** (10 μM) (in these experiments, "Twinlight" apparatus was used to irradiate many HeLa-S3 cells at the same time in a well). Figure 11d−f displays a brightfield image, an PI emission image, and an overlay image after photoirradiation at 465 nm for 10 min in the absence of **5**. Figure 11g−i shows microscopic images, and an overlay image without photoirradiation in the presence of **5** (10 μM). These data suggest that the photoirradiation of **5** mainly induces necrosis-like cell death of HeLa-S3 cells.

dx.doi.org/10.1021/ic402387b | *Inorg. Chem.* 2014, 53, 409−422

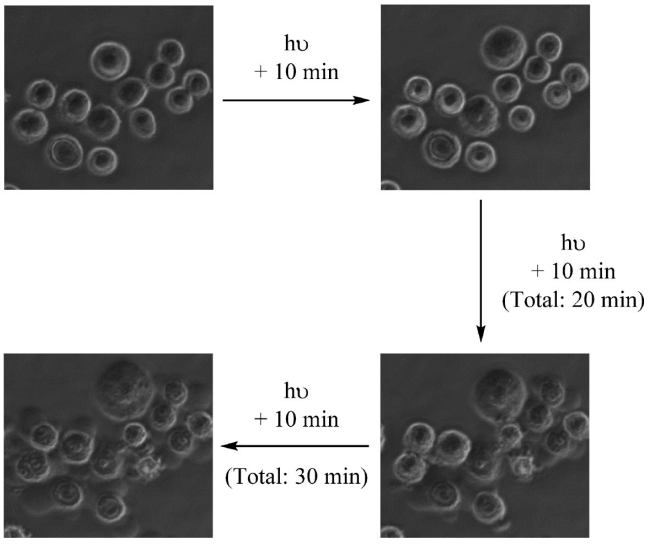

Figure 10. Luminescence microscope images (BIOREVO BZ-9000, Keyence) showing membrane swelling of HeLa-S3 cells (×40) upon photoirradiation at 470 nm in the presence of **5** (10 μM).

Moreover, it was strongly indicated that **5** induces cell death more efficiently than **4** (Figure11j–l vs Figure 11a–c), as summarized in Figure 12. According to our previous method,[12] the intracellular concentration of **5** was determined by ICP-AES to be 0.14 ± 0.03 fmol/cell, which is almost identical to that of **4** (0.16 ± 0.03 fmol/cell).[40] These facts allowed us to conclude that H_3·**5** and acid-free **5** generate $^1O_2$ much more efficiently than **4** (and its protonated form) not only in a flask (see Figure 7) but also in living cells. It is likely that the cell death would be triggered by the damage of not only mitochondria but also other organella.

Annexin V-Cy3 staining of HeLa-S3 cells was also investigated, and these results are shown in Supporting Information, Figure S17, in which the red-colored emission from Annexin V-Cy3 was scarcely observed when **5** was used (Supporting Information, Figure S17b), which is different from the behavior of **4** (Supporting Information, Figure S17d). These data may suggest that mechanisms of cell death induced by photoirradiation of **4** and **5** are somehow different and/or that cell death caused by **5** is much faster than by **4**.

It is described that singlet oxygen is not only toxic to cells but also is capable of inducing a cellular stress response.[41] Therefore, we do not exclude the possibility that the cell death is triggered not only by photoinduced oxidation of methionine, cysteine, tryptophan, and other amino acid residues of intracellular proteins and enzymes but also by the activation of a stress-related signal pathway.

CONCLUSIONS

We report herein on the design, synthesis, characterization, photochemical properties, cellular imaging, and photosensitization activity of pH-responsive Ir(III) complexes **5**, **6**, **7**, and **8** having three pyridyl groups, the luminescent behavior of which were predicted based on DFT calculations. The luminescence emissions of these complexes in DMSO were found to be strongly green colored at wavelengths around 500 nm. The acidification of **5** and **7** induced a significant red-shift, and their emission intensity was dramatically decreased, because of the protonation of the three pyridyl groups. This behavior is opposite to that of **3** and **4**.[12] In the case of **6** and **8**, the

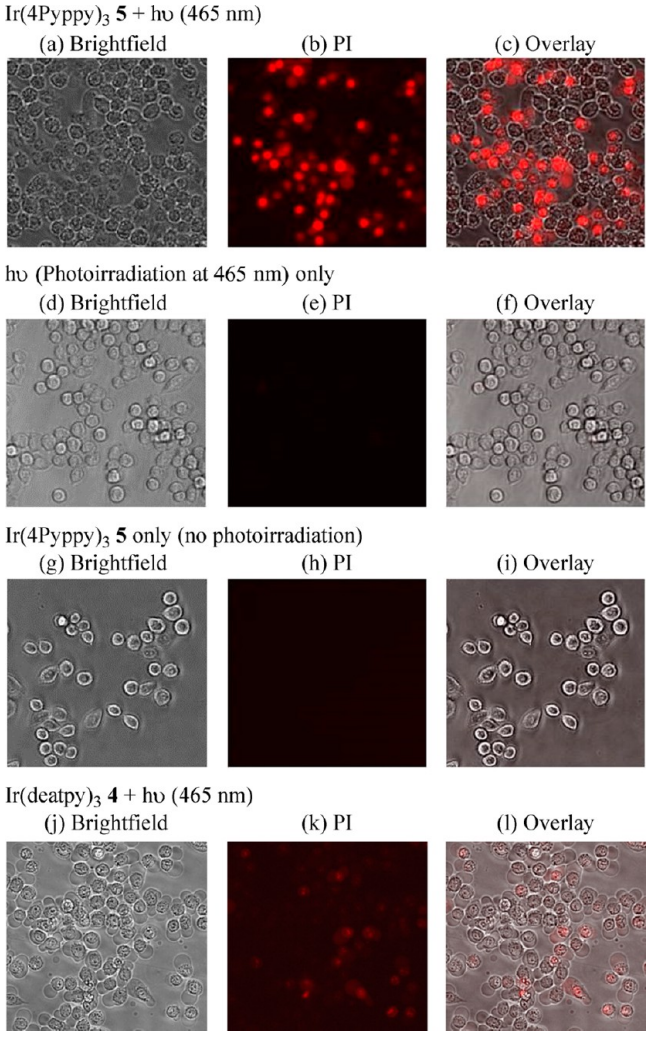

Figure 11. Fluorescence microscope images (BIOREVO BZ-9000, Keyence) of HeLa-S3 cells (×20) (a)–(c) and (j)–(l) irradiated at 465 nm (Twinlight, RELYON) for 10 min after preincubation for 30 min with **5** or **4** (10 μM), (d)–(f) irradiated for 10 min after preincubation for 30 min with only DMSO, (g)–(i) incubated for 30 min with **5** (10 μM), then washed and stained with PI (30 μM) for 30 min. Excitation at 540 nm to observe PI. (a), (d), (g), and (j) brightfield images of HeLa-S3, (b), (e), (h), and (b) emission images of PI, (c) overlay image (a) and (b), (f) overlay image (d) and (e), (i) overlay image (g) and (h), (l) overlay image of (j) and (k).

addition of acid induced a decrease in emission intensity with a negligible change in the emission wavelength. A detailed theoretical study involving DFT calculations suggested that the protonation of the pyridyl groups caused new ^{3}MLCT transition (from the phenyl π and Ir d orbitals to protonated pyridine rings) and ^{3}ILCT transitions which induced a significant red-shift in their emission.

Generation of $^1O_2$ by photoirradiation of **5** and **6** was confirmed by the oxidation of TPC, which was monitored by ESR measurements, and the oxidation of thioanisole to the corresponding sulfoxide was followed by ^{1}H NMR. In addition, it was found that the generation of $^1O_2$ was facilitated under neutral to basic condition rather than acidic conditions, as confirmed by the decomposition of DPBF. The catalytic photooxidation reaction of thioanisole proceeded efficiently with 0.1 mol % of **5** or **6**. A cellular imaging study of HeLa-S3 cells with **5**, LysoTracker and MitoTracker showed the

dx.doi.org/10.1021/ic402387b | Inorg. Chem. 2014, 53, 409–422

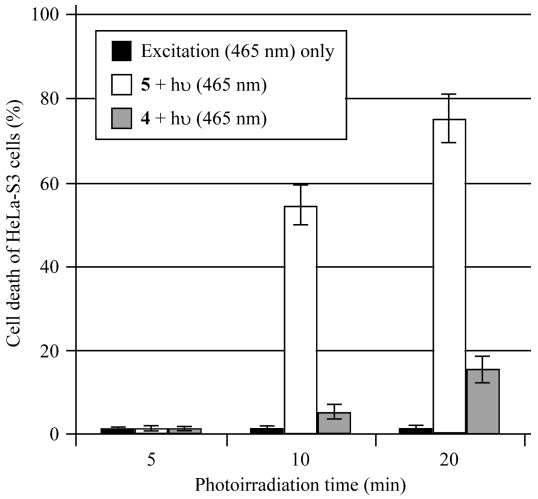

Figure 12. Cell death of HeLa-S3 cells upon photoirradiation at 465 nm in the absence (filled bar) and in the presence of **5** (10 μM) (open bar) and **4** (10 μM) (faded bar) in MEM/DMSO (99/1) (monitored by PI-staining). Cell death of HeLa-S3 cells (%) = (number of cells stained by PI/number of all cells) × 100.

emission of **5** occurred largely in mitochondria. The photoirradiation of **5** induced the cell death of HeLa-S3 cells, possibly via necrosis-like cell death. There is a possibility that the cell death was triggered by the damage not only in mitochondria but also in other organelles, because of efficient $^1O_2$ generation by the free form and protonated form of **5**.[42]

Our results provide useful information for the future design and synthesis of new pH-responsive Ir complexes and their applications to photocatalytic reactions, biological chemistry, medicinal chemistry,[43] and related fields.

■ ASSOCIATED CONTENT

Supporting Information

Further details are provided in Figures S1−S13 and Table S1. This material is available free of charge via the Internet at http://pubs.acs.org.

■ AUTHOR INFORMATION

Corresponding Author

*E-mail: shinaoki@rs.noda.tus.ac.jp.

Notes

The authors declare no competing financial interest.

■ ACKNOWLEDGMENTS

This work was supported by grants-in-aid from the Ministry of Education, Culture, Sports, Science, and Technology (MEXT) of Japan (Nos. 22390005, 22659005, and 24659011 for S.A. and Nos. 22890200 and 24890256 for Y.H.) and High-Tech Research Center Project for Private Universities (matching fund subsidy from MEXT). We appreciate the aid of Mrs. Fukiko Hasegawa (Faculty of Pharmaceutical Sciences, Tokyo University of Science) for collecting and interpreting the mass spectra of the Ir complexes. We thank Prof. Ryo Abe and Dr. Toshihiro Suzuki (Research Institute for Biomedical Sciences, Tokyo University of Science) for the helpful discussion and the preparation for the HeLa-S3 cells.

■ REFERENCES

(1) (a) Sprouse, S.; King, K. A.; Spellane, P. J.; Watts, R. J. *J. Am. Chem. Soc.* **1984**, *106*, 6647−6653. (b) King, K. A.; Spellane, P. J.; Watts, R. J. *J. Am. Chem. Soc.* **1985**, *107*, 1431−1432. (c) Garces, F. O.; King, K. A.; Watts, R. J. *Inorg. Chem.* **1988**, *27*, 3464−3471. (d) Dedeian, K.; Djurovich, P. I.; Garces, F. O.; Carlson, G.; Watts, R. J. *Inorg. Chem.* **1991**, *30*, 1685−1687. (e) Carlson, G. A.; Djurovich, P. I.; Watts, R. J. *Inorg. Chem.* **1993**, *32*, 4483−4484. (f) Schmid, B.; Garces, F. O.; Watts, R. J. *Inorg. Chem.* **1994**, *33*, 9−14. (g) Lamansky, S.; Djurovich, P.; Murphy, D.; Abdel-Razzaq, F.; Kwong, R.; Tsyba, I.; Bortz, M.; Mui, B.; Bau, R.; Thompson, M. E. *Inorg. Chem.* **2001**, *40*, 1704−1711. (h) Tamayo, A. B.; Alleyne, B. D.; Djurovich, P. I.; Lamansky, S.; Tsyba, I.; Ho, N. N.; Bau, R.; Thompson, M. E. *J. Am. Chem. Soc.* **2003**, *125*, 7377−7387. (i) Lowry, M. S.; Hudson, W. R.; Pascal, R. A., Jr.; Bernhard, S. *J. Am. Chem. Soc.* **2004**, *126*, 14129−14135. (j) Obara, S.; Itabashi, M.; Okuda, F.; Tamaki, S.; Tanabe, Y.; Ishii, Y.; Nozaki, K.; Haga, M. *Inorg. Chem.* **2006**, *45*, 8907−8921. (k) Flamigni, L.; Barbieri, A.; Sabatini, C.; Ventura, B.; Barigelletti, F. *Top. Curr. Chem.* **2007**, *281*, 143−203. (l) Wong, W.-Y.; Ho, C.-L. *Coord. Chem. Rev.* **2009**, *253*, 1709−1758. (m) Chi, Y.; Chou, P.-T. *Chem. Soc. Rev.* **2010**, *39*, 638−655.

(2) (a) Colombo, M. G.; Brunold, T. C.; Riedener, T.; Güdel, H. U. *Inorg. Chem.* **1994**, *33*, 545−550. (b) Tang, K.-C.; Liu, K. L.; Chen, I.-C. *Chem. Phys. Lett.* **2004**, *386*, 437−441. (c) Hedley, G. J.; Ruseckas, A.; Samuel, I. D. W. *J. Phys. Chem. A* **2010**, *114*, 8961−8968.

(3) (a) Grushin, V. V.; Herron, N.; LeCloux, D. D.; Marshall, W. J.; Petrov, V. A.; Wang, Y. *Chem. Commun.* **2001**, *16*, 1494−1495. (b) You, Y.; Park, S. Y. *J. Am. Chem. Soc.* **2005**, *127*, 12438−12439. (c) Li, J.; Djurovich, P. I.; Alleyne, B. D.; Yousufuddin, M.; Ho, N. N.; Thomas, J. C.; Peters, J. C.; Bau, R.; Thompson, M. E. *Inorg. Chem.* **2005**, *44*, 1713−1727. (d) Hwang, F.-M.; Chen, H.-Y.; Chen, P.-S.; Liu, C.-S.; Chi, Y.; Shu, C.-F.; Wu, F.-I.; Chou, P.-T.; Peng, S.-M.; Lee, G.-H. *Inorg. Chem.* **2005**, *44*, 1344−1353. (e) Lowry, M. S.; Bernhard, S. *Chem.—Eur. J.* **2006**, *12*, 7970−7977. (f) Kim, E.; Park, S. B. *Chem.—Asian J.* **2009**, *4*, 1646−1658. (g) Ladouceur, S.; Fortin, D.; Zysman-Colman, E. *Inorg. Chem.* **2011**, *50*, 11514−11526. (h) Zaarour, M.; Singh, A.; Latouche, C.; Williams, J. A. G.; Ledoux-Rak, I.; Zyss, J.; Boucekkine, A.; Bozec, H. L.; Guerchais, V.; Dragonetti, C.; Colombo, A.; Roberto, D.; Valore, A. *Inorg. Chem.* **2013**, *52*, 7987−7994.

(4) (a) Baldo, M. A.; O'Brien, D. F.; You, Y.; Shoustikov, A.; Sibley, S.; Thompson, M. E.; Forrest, S. R. *Nature* **1998**, *395*, 151−154. (b) Lamansky, S.; Djurovich, P.; Murphy, D.; Abdel-Razzaq, F.; Lee, H.-E.; Adachi, C.; Burrows, P. E.; Forrest, S. R.; Thompson, M. E. *J. Am. Chem. Soc.* **2001**, *123*, 4304−4312. (c) Nazeeruddin, M. K.; Humphry-Baker, R.; Berner, D.; Rivier, S.; Zuppiroli, L.; Graetzel, M. *J. Am. Chem. Soc.* **2003**, *125*, 8790−8797. (d) Tsuboyama, A.; Iwawaki, H.; Furugori, M.; Mukaide, T.; Kamatani, J.; Igawa, S.; Moriyama, T.; Miura, S.; Takiguchi, T.; Okada, S.; Hoshino, M.; Ueno, K. *J. Am. Chem. Soc.* **2003**, *125*, 12971−12979. (e) D'Andrade, B. W.; Forrest, S. R. *Adv. Mater.* **2004**, *16*, 1585−1595. (f) Jung, S.; Kang, Y.; Kim, H.-S.; Kim, Y.-H.; Lee, C.-L.; Kim, J.-J.; Lee, S.-K.; Kwon, S.-K. *Eur. J. Inorg. Chem.* **2004**, *17*, 3415−3423. (g) Okada, S.; Okinaka, K.; Iwawaki, H.; Furugori, M.; Hashimoto, M.; Mukaide, T.; Kamatani, J.; Igawa, S.; Tsuboyama, A.; Takiguchi, T.; Ueno, K. *Dalton Trans.* **2005**, *34*, 1583−1590. (h) Holder, E.; Langeveld, B. M. W.; Schubert, U. S. *Adv. Mater.* **2005**, *17*, 1109−1121. (i) Evans, R. C.; Douglas, P.; Winscom, C. J. *Coord. Chem. Rev.* **2006**, *250*, 2093−2126. (j) Song, Y.-H.; Chiu, Y.-C.; Chi, Y.; Cheng, Y.-M.; Lai, C.-H.; Chou, P.-T.; Wong, K.-T.; Tsai, M.-H.; Wu, C.-C. *Chem.—Eur. J.* **2008**, *14*, 5423−5434. (k) Wong, W.-Y.; Ho, C.-L. *J. Mater. Chem.* **2009**, *19*, 4457−4482. (l) Ulbricht, C.; Beyer, B.; Friebe, C.; Winter, A.; Schubert, U. S. *Adv. Mater.* **2009**, *21*, 4418−4441. (m) Farinola, G. M.; Ragni, R. *Chem. Soc. Rev.* **2011**, *40*, 3467−3482. (n) Sasabe, H.; Kido, J. *Chem. Mater.* **2011**, *23*, 621−630. (o) Margapoti, E.; Muccini, M.; Sharma, A.; Colombo, A.; Dragonetti, C.; Roberto, D.; Valore, A. *Dalton Trans.* **2012**, *41*, 9227−9231.

(5) (a) Goodall, W.; Williams, J. A. G. *J. Chem. Soc., Dalton Trans.* **2000**, 2893−2895. (b) Ho, M.-L.; Hwang, F.-M.; Chen, P.-N.; Hu, Y.-H.; Cheng, Y.-M.; Chen, K.-S.; Lee, G.-H.; Chi, Y.; Chou, P.-T. *Org.*

Biomol. Chem. **2006**, *4*, 98−103. (c) Konishi, K.; Yamaguchi, H.; Harada, A. *Chem. Lett.* **2006**, *35*, 720−721. (d) Schmittel, M.; Lin, H. *Inorg. Chem.* **2007**, *46*, 9139−9145. (e) Zhao, Q.; Cao, T.; Li, F.; Li, X.; Jing, H.; Yi, T.; Huang, C. *Organometallics* **2007**, *26*, 2077−2081. (f) Zhao, Q.; Liu, S.; Shi, M.; Li, F.; Jing, H.; Yi, T.; Huang, C. *Organometallics* **2007**, *26*, 5922−5930. (g) Zhao, N.; Wu, Y.-H.; Wen, H.-M.; Zhang, X.; Chen, Z.-N. *Organometallics* **2009**, *28*, 5603−5611. (h) Zhao, Q.; Li, F.; Huang, C. *Chem. Soc. Rev.* **2010**, *39*, 3007−3030. (i) Araya, J. C.; Gajardo, J.; Moya, S. A.; Aguirre, P.; Toupet, L.; Williams, J. A. G.; Escadeillas, M.; Bozec, H. L.; Guerchais, V. *New. J. Chem.* **2010**, *34*, 21−24. (j) Brandel, J.; Sairenji, M.; Ichikawa, K.; Nabeshima, T. *Chem. Commun.* **2010**, *46*, 3958−3960. (k) Guerchais, V.; Fillaut, J.-L. *Coord. Chem. Rev.* **2011**, *255*, 2448−2457. (l) You, Y.; Han, Y.; Lee, Y.-M.; Park, S. Y.; Nam, W.; Lippard, S. J. *J. Am. Chem. Soc.* **2011**, *133*, 11488−11491.

(6) Nagib, D. A.; Scott, M. E.; MacMillan, D. W. C. *J. Am. Chem. Soc.* **2009**, *131*, 10875−10877.

(7) (a) Lo, K. K.-W.; Chung, C.-K.; Lee, T. K.-M.; Lui, L.-H.; Tsang, K. H.-K.; Zhu, N. *Inorg. Chem.* **2003**, *42*, 6886−6897. (b) Lo, K. K.-W.; Lee, P.-K.; Lau, J. S.-Y. *Organometallics* **2008**, *27*, 2998−3006. (c) Lo, K. K.-W.; Louie, M.-W.; Zhang, K. Y. *Coord. Chem. Rev.* **2010**, *254*, 2603−2622. (d) Zhang, S.; Hosaka, M.; Yoshihara, T.; Negishi, K.; Iida, Y.; Tobita, S.; Takeuchi, T. *Cancer Res.* **2010**, *70*, 4490−4498. (e) Zhang, K. Y.; Li, S. P.-Y.; Zhu, N.; Or, I. W.-S.; Cheung, M. S.-H.; Lam, Y.-W.; Lo, K. K.-W. *Inorg. Chem.* **2010**, *49*, 2530−2540. (f) Leung, S.-K.; Kwok, K. Y.; Zhang, K. Y.; Lo, K. K.-W. *Inorg. Chem.* **2010**, *49*, 4984−4995. (g) Zhang, K. Y.; Liu, H.-W.; Fong, T. T.-H.; Chen, X.-G.; Lo, K. K.-W. *Inorg. Chem.* **2010**, *49*, 5432−5443. (h) Zhao, Q.; Yu, M.; Shi, L.; Liu, S.; Li, C.; Shi, M.; Zhou, Z.; Huang, C.; Li, F. *Organometallics* **2010**, *29*, 1085−1091. (i) Zhao, Q.; Huang, C.; Li, F. *Chem. Soc. Rev.* **2011**, *40*, 2508−2524. (j) Lo, K. K.-W.; Li, S. P.-Y.; Zhang, K. Y. *New. J. Chem.* **2011**, *35*, 265−287. (k) Wu, H.; Yang, T.; Zhao, Q.; Zhou, J.; Li, C.; Li, F. *Dalton Trans.* **2011**, *40*, 1969−1976. (l) Lee, P.-K.; Liu, H.-W.; Yiu, S.-M.; Louie, M.-W.; Lo, K. K.-W. *Dalton Trans.* **2011**, *40*, 2180−2189. (m) Li, C.; Yu, M.; Sun, Y.; Wu, Y.; Huang, C.; Li, F. *J. Am. Chem. Soc.* **2011**, *133*, 11231−11239. (n) You, Y.; Han, Y.; Lee, Y.-M.; Park, S. Y.; Nam, W.; Lippard, S. J. *J. Am. Chem. Soc.* **2011**, *133*, 11488−11491. (o) You, Y.; Lee, S.; Kim, T.; Ohkubo, K.; Chae, W.-S.; Fukuzumi, S.; Jhon, G.-J.; Nam, W.; Lippard, S. J. *J. Am. Chem. Soc.* **2011**, *133*, 18328−18342. (p) Lee, P.-K.; Law, W. H.-T.; Liu, H.-W.; Lo, K. K.-W. *Inorg. Chem.* **2011**, *50*, 8570−8579. (q) Wu, Y.; Jing, H.; Dong, Z.; Zhao, Q.; Wu, H.; Li, F. *Inorg. Chem.* **2011**, *50*, 7412−7420. (r) Baggaley, E.; Weinstein, J. A.; Williams, J. A. G. *Coord. Chem. Rev.* **2012**, *256*, 1762−1785. (s) Patra, M.; Gasser, G. *ChemBioChem* **2012**, *13*, 1232−1252. (t) You, Y.; Cho, S.; Nam, W. *Inorg. Chem.* **2013**, DOI: 10.1021/ic4013872.

(8) Aoki, S.; Matsuo, Y.; Ogura, S.; Ohwada, H.; Hisamatsu, Y.; Moromizato, S.; Shiro, M.; Kitamura, M. *Inorg. Chem.* **2011**, *50*, 806−818.

(9) Hisamatsu, Y.; Aoki, S. *Eur. J. Inorg. Chem.* **2011**, *35*, 5360−5369.

(10) For the other examples of the substitution reactions of cyclometalated complexes, see: (a) Qin, T.; Ding, J.; Wang, L.; Baumgarten, M.; Zhou, G.; Mullen, K. *J. Am. Chem. Soc.* **2009**, *131*, 14329−14336. (b) Cheung, K.-M.; Zhang, Q.-F.; Chan, K.-W.; Lam, M. H. W.; Williams, I. D.; Leung, W.-H. *J. Organomet. Chem.* **2005**, *690*, 2913−2921.

(11) For different types of pH probes based on Ir(III) complexes have been reported, see: (a) Goldstein, D. C.; Cheng, Y. Y.; Schmidt, T. W.; Bhadbhade, M.; Thordarson, P. *Dalton Trans.* **2011**, *40*, 2053−2061. (b) Weng, J.; Mei, Q.; Jiang, W.; Fan, Q.; Tong, B.; Ling, Q.; Huang, W. *Analyst* **2013**, *138*, 1689−1699.

(12) Moromizato, S.; Hisamatsu, Y.; Suzuki, T.; Matsuo, Y.; Abe, R.; Aoki, S. *Inorg. Chem.* **2012**, *51*, 12697−12706.

(13) Some groups have reported on cyclometalated Ir(III) complexes as efficient singlet oxygen sensitizers, see: (a) Gao, R.; Ho, D. G.; Hernandez, B.; Selke, M.; Murphy, D.; Djurovich, P. I.; Thompson, M. E. *J. Am. Chem. Soc.* **2002**, *124*, 14828−14829. (b) Djurovich, P. I.; Murphy, D.; Thompson, M. E.; Hernandez, B.; Gao, R.; Hunt, P. L.; Selke, M. *Dalton Trans.* **2007**, *34*, 3763−3770. (c) Takizawa, S.; Aboshi, R.; Murata, S. *Photochem. Photobiol. Sci.* **2011**, *10*, 895−903. (d) Sun, J.; Zhao, J.; Guo, H.; Wu, W. *Chem. Commun.* **2012**, *48*, 4169−4171.

(14) pH-sensitive Ir(III) complexes having nitrogenous heterocyclic substituents at cyclometalated ligands have been reported by some groups. See: (a) Licini, M.; Williams, J. A. G. *Chem. Commun.* **1999**, 1943−1944. (b) Arm, K. J.; Leslie, W.; Williams, J. A. G. *Inorg. Chim. Acta* **2006**, *359*, 1222−1232. (c) Murphy, L.; Congreve, A.; Pälsson, L.-O.; Williams, J. A. G. *Chem. Commun.* **2010**, *46*, 8743−8745. (d) Chen, Y.; Zhang, A.; Liu, Y.; Wang, K. *J. Organomet. Chem.* **2011**, *696*, 1716−1722.

(15) Frisch, M. J.; Trucks, G. W.; Schlegel, H. B.; Scuseria, G. E.; Robb, M. A.; Cheeseman, J. R.; Montgomery, J. A.; Vreven, Jr., T.; Kudin, K. N.; Burant, J. C.; Millam, J. M.; Iyengar, S. S.; Tomasi, J.; Barone, V.; Mennucci, B.; Cossi, M.; Scalmani, G.; Rega, N.; Petersson, G. A.; Nakatsuji, H.; Hada, M.; Ehara, M.; Toyota, K.; Fukuda, R.; Hasegawa, J. Ishida, M.; Nakajima, T.; Honda, Y.; Kitao, O.; Nakai, H.; Klene, M.; Li, X.; Knox, J. E.; Hratchian, H. P.; Cross, J. B.; Bakken, V.; Adamo, C.; Jaramillo, J.; Gomperts, R.; Stratmann, R. E.; Yazyev, O.; Austin, A. J.; Cammi, R.; Pomelli, C.; Ochterski, J. W.; Ayala, P. Y.; Morokuma, K.; Voth, G. A.; Salvador, P.; Dannenberg, J. J.; Zakrzewski, V. G.; Dapprich, S.; Daniels, A. D.; Strain, M. C.; Farkas, O.; Malick, D. K.; Rabuck, A. D.; Raghavachari, K.; Foresman, J. B.; Ortiz, J. V.; Cui, Q.; Baboul, A. G.; Clifford, S.; Cioslowski, J.; Stefanov, B. B.; Liu, G.; Liashenko, A.; Piskorz, P.; Komaromi, I.; Martin, R. L.; Fox, D. J.; Keith, T.; Al-Laham, M. A.; Peng, C. Y.; Nanayakkara, A.; Challacombe, M.; Gill, P. M. W.; Johnson, B.; Chen, W.; Wong, M. W.; Gonzalez, C.; Pople, J. A. *Gaussian 03*, Revision C.02; Gaussian, Inc.: Wallingford, CT, 2004.

(16) You, Y.; Nam, W. *Chem. Soc. Rev.* **2012**, *41*, 7061−7084.

(17) After we started this work, the same compounds and several derivatives have become public from a patent from Kido and co-workers, although pH-dependent photochemical properties and biological application were not described. See: Osachi, Y.; Kido, J.; Watanabe, M.; Takeda, T. *Jpn. Kokai Tokkyo Koho* 2012, JP 2012167028 A 20120906.

(18) (a) DeRosa, M. C.; Crutchley, R. J. *Coord. Chem. Rev.* **2002**, *233*−*234*, 351−371. (b) Clennan, E. L.; Pace, A. *Tetrahedron* **2005**, *61*, 6665−6691.

(19) Konno, H.; Sasaki, Y. *Chem. Lett.* **2003**, *32*, 252−253.

(20) (a) Miyaura, N.; Suzuki, A. *Chem. Rev.* **1995**, *95*, 2457−2483. (b) Caddick, S. *Tetrahedron* **1995**, *51*, 10403−10432. (c) Yi, C.; Blum, C.; Lehmann, M.; Keller, S.; Liu, S.-X.; Frei, G.; Neels, A.; Hauser, J.; Schürch, S.; Decurtins, S. *J. Org. Chem.* **2010**, *75*, 3350−3357. (d) Suzuki, A.; Brown, H. C. *Organic Synthesis via Boranes*; Aldrich Chemical Company:: Milwaukee, WI, 2003; Vol. *3*, Suzuki Coupling.

(21) (a) Wright, S. W.; Hageman, D. L.; McClure, L. D. *J. Org. Chem.* **1994**, *59*, 6095−6097. (b) Ihm, C.; Ko, Y.-J.; Shin, J.-H.; Paek, K. *Tetrahedron Lett.* **2006**, *47*, 8847−8850.

(22) Edkins, R. M.; Bettington, S. L.; Goeta, A. E.; Beeby, A. *Dalton Trans.* **2011**, *40*, 12765−12770.

(23) Nakamura, K.; Ishiyama, K.; Ikai, H.; Kanno, T.; Sasaki, K.; Niwano, Y.; Kohno, M. *J. Clin. Biochem. Nutr.* **2011**, *49*, 87−95.

(24) It is considered that the protonation of the nitrogen atom of the ppym ligand is negligible, based on the fact that the addition of H^+ to **9** ($Ir(ppym)_3$ in Chart 4) induced a negligible change in its UV/vis and emission spectra (data not shown).

(25) UV/vis spectra of **5** and **6** in degassed DMSO/buffer (from pH 4 to 10) solution at 298 K are shown in Supporting Information, Figure S5 and S6.

(26) UV/vis spectra of **7** in degassed DMSO/buffer (from pH 4 to 10) at 298 K are shown in Supporting Information, Figure S8.

(27) (a) Colombo, M. G.; Hauser, A.; Güdel, H. U. *Inorg. Chem.* **1993**, *32*, 3088−3092. (b) Hay, P. J. *J. Phys. Chem. A* **2002**, *106*, 1634−1641. (c) Hedley, G. J.; Ruseckas, A.; Samuel, I. D. W. *Chem. Phys. Lett.* **2008**, *450*, 292−296. (d) You, Y.; Park, S. Y. *Dalton Trans.* **2009**, *38*, 1267−1282. (e) Hofbeck, T.; Yersin, H. *Inorg. Chem.* **2010**, *49*, 9290−9299. (f) Fantacci, S.; Angelis, F. D. *Coord. Chem. Rev.* **2011**, *255*, 2704−2726.

(28) Thompson, A. M. W. C.; Smailes, M. C. C.; Jeffery, J. C.; Ward, M. D. *J. Chem. Soc., Dalton Trans.* **1997**, 737−743.
(29) (a) Bonneau, R.; Pottier, R.; Bagno, O.; Joussot-Dubien, J. *Photochem. Photobiol.* **1975**, *21*, 159−163. (b) Pottier, R.; Bonneau, R.; Joussot-Dubien, J. *Photochem. Photobiol.* **1975**, *22*, 59−61. (c) Han, J.; Burgess, K. *Chem. Rev.* **2010**, *110*, 2709−2728. (d) Lovell, J. F.; Liu, T. W. B.; Chen, J.; Zheng, G. *Chem. Rev.* **2010**, *110*, 2839−2857.
(30) (a) Foote, C. S.; Peters, J. W. *J. Am. Chem. Soc.* **1971**, *93*, 3795−3796. (b) Gu, C.-L.; Foote, C. S.; Kacher, M. L. *J. Am. Chem. Soc.* **1981**, *103*, 5949−5951. (c) Liang, J.-J.; Gu, C.-L.; Kacher, M. L.; Foote, C. S. *J. Am. Chem. Soc.* **1983**, *105*, 4717−4721. (d) Ishiguro, K.; Hayashi, M.; Sawaki, Y. *J. Am. Chem. Soc.* **1996**, *118*, 7265−7271. (e) Jensen, F.; Greer, A.; Clennan, E. L. *J. Am. Chem. Soc.* **1998**, *120*, 4439−4449. (f) Clennan, E. L. *Acc. Chem. Res.* **2001**, *34*, 875−884. (g) Baciocchi, E.; Giacco, T. D.; Elisei, F.; Gerini, M. F.; Guerra, M.; Lapi, A.; Liberali, P. *J. Am. Chem. Soc.* **2003**, *125*, 16444−16454. (h) Bonesi, S. M.; Manet, I.; Freccero, M.; Fagnoni, M.; Albini, A. *Chem.—Eur. J.* **2006**, *12*, 4844−4857. (i) Dad'ová, J.; Svobodová, E.; Sikorski, M.; König, B.; Cibulka, R. *ChemCatChem* **2012**, *4*, 620−623.
(31) It is considered that the concentration of thioanisole oxide formed by photoreaction is higher than that of dissolved oxygen. In these experiments, fresh air was taken into the reaction mixture by opening the cap at every photoreaction, which might supply sufficient oxygen for the oxidation reaction to reach completion.
(32) (a) Li, M. Y.; Cline, C. S.; Koker, E. B.; Carmichael, H. H.; Chignell, C. F.; Bilski, P. *Photochem. Photobiol.* **2001**, *74*, 760−764. (b) Bancirova, M. *Luminescence* **2011**, *26*, 685−688.
(33) Howard, J. A.; Mendenhall, G. D. *Can. J. Chem.* **1975**, *53*, 2199−2201.
(34) The lifetimes of **4** and H_3·**4** were reported to be 2.9 and 1.9 μs in our previous paper (ref 12), implying that the lifetime of **4** was decreased by the protonation, albeit H_3·**4** has a greater HOMO−LUMO gap and generates $^1O_2$ more efficiently than acid-free **4**. These data allowed us to consider that the efficiency of $^1O_2$ generation is regulated by the HOMO−LUMO energy gap rather than the lifetime of Ir complexes, at least on the microsecond time scale.
(35) Carloni, P.; Damiani, E.; Greci, L.; Stipa, P.; Tanfani, F.; Tartaglini, E. *Res. Chem. Intermed.* **1993**, *19*, 395−405.
(36) Under experimental conditions, Ir complexes converged dissolved oxygen to $^1O_2$, and the concentration of dissolved oxygen is roughly estimated 170−200 μM (Fujinaga, T.; Izutsu, K.; Adachi, T. *Bull. Chem. Soc. Jpn.* **1969**, *42*, 140−145), which may reflect with the generation of nitroxide radical..
(37) Demaurex, N. *News Physiol. Sci.* **2002**, *17*, 1−5.
(38) Orij, R.; Postmus, J.; Beek, A. T.; Brul, S.; Smits, G. J. *Microbiology* **2009**, *155*, 268−278.
(39) Galluzzi, L.; Vitale, L.; Abrams, J. M.; Alnemri, E. S.; Baehrecke, E. H.; Blagosklonny, M. V.; Dawson, T. M.; Dawson, V. L.; El-Deiry, W. S.; Fulda, S.; Gottlieb, E.; Green, D. R.; Hengartner, M. O.; Kepp, O.; Knight, R. A.; Kumar, S.; Lipton, S. A.; Lu, X.; Madeo, F.; Malorni, W.; Mehlen, P.; Nunez, G.; Peter, M. E.; Piacentini, M.; Rubinsztein, D. C.; Shi, Y.; Simon, H.-U.; Vandenabeele, P.; White, E.; Yuan, J.; Zhivotovsky, B.; Melino, G.; Kroemer, G. *Cell Death Differ.* **2012**, *19*, 107−120.
(40) In our previous report (ref 12), the intracellular concentration of **4** in HeLa-S3 cells was determined to be 0.20 ± 0.03 fmol/cell. We assume that these values are within experimental errors (the concentration of **1** ($Ir(ppy)_3$) was determined to be 0.23 ± 0.03 fmol/cell in this work, which is similar to the reported value for **2** (0.27 ± 0.03 fmol/cell) (ref 12)).
(41) (a) Davies, M. J. *Biochem. Biophys. Res. Commun.* **2003**, *305*, 761−770. (b) Klotz, L.-O.; Kröncke, K.-D.; Sies, H. *Photochem. Photobiol. Sci.* **2003**, *2*, 88−94.
(42) Recently, we succeed in the synthesis of the 2-pyridyl analogue of **5** and **6**, and its photochemical behaviors will reported elsewhere.
(43) (a) Gorman, A.; Killoran, J.; O'Shea, C.; Kenna, T.; Gallagher, W. M.; O'Shea, D. F. *J. Am. Chem. Soc.* **2004**, *126*, 10619−10631. (b) McDonnell, S. O.; Hall, M. J.; Allen, L. T.; Byrne, A.; Gallagher, W. M.; O'Shea, D. F. *J. Am. Chem. Soc.* **2005**, *127*, 16360−16361. (c) Yogo, T.; Urano, Y.; Mizushima, A.; Sunahara, H.; Inoue, T.; Hirose, K.; Iino, M.; Kikuchi, K.; Nagano, T. *Proc. Natl. Acad. Sci. U.S.A.* **2008**, *105*, 28−32.